

1 **A UNIFIED ANALYSIS FRAMEWORK FOR ITERATIVE**
2 **PARALLEL-IN-TIME ALGORITHMS** *

3 MARTIN J. GANDER[†], THIBAUT LUNET[‡], DANIEL RUPRECHT[‡], AND ROBERT
4 SPECK[§]

5 **Abstract.** Parallel-in-time integration has been the focus of intensive research efforts over
6 the past two decades due to the advent of massively parallel computer architectures and the scaling
7 limits of purely spatial parallelization. Various iterative parallel-in-time (PinT) algorithms have been
8 proposed, like PARAREAL, PFASST, MGRIT, and Space-Time Multi-Grid (STMG). These methods
9 have been described using different notations, and the convergence estimates that are available are
10 difficult to compare. We describe PARAREAL, PFASST, MGRIT and STMG for the Dahlquist
11 model problem using a common notation and give precise convergence estimates using generating
12 functions. This allows us, for the first time, to directly compare their convergence. We prove that all
13 four methods eventually converge super-linearly, and also compare them numerically. The generating
14 function framework provides further opportunities to explore and analyze existing and new methods.

15 **Key words.** Parallel in Time (PinT) methods, PARAREAL, PFASST, MGRIT, space-time
16 multi-grid (STMG), generating functions, convergence estimates.

17 **AMS subject classifications.** 65R20, 45L05, 65L20

18 **1. Introduction.** The efficient numerical solution of time-dependent ordinary
19 and partial differential equations (ODEs/PDEs) has always been an important re-
20 search subject in computational science and engineering. Nowadays, with high-
21 performance computing platforms providing more and more processors whose indi-
22 vidual processing speeds are no longer increasing, the capacity of algorithms to run
23 concurrently becomes important. As classical parallelization algorithms start to reach
24 their intrinsic efficiency limits, substantial research efforts have been invested to find
25 new parallelization approaches that can translate the computing power of modern
26 many-core high-performance computing architectures into faster simulations.

27 For time-dependent problems, the idea to parallelize across the time direction
28 has gained renewed attention in the last two decades¹. Various algorithms have been
29 developed, for overviews see the papers by Gander [18] or Ong and Schroder [41].
30 Four iterative algorithms have received significant attention, namely PARAREAL [36]
31 (426 citat. since 2001)², the *Parallel Full Approximation Scheme in Space and Time*
32 (PFASST) [11] (228 citat. since 2012), *Multi-Grid Reduction In Time*, (MGRIT) [16,
33 14] (238 citat. since 2014) and a specific form of *Space-Time Multi-Grid* (STMG) [25]
34 (122 citat. since 2016). Other algorithms have been proposed, *e.g.* the *Parallel (or*
35 *PARAREAL) Implicit Time integration Algorithm* PITA [15] (264 citat. since 2003)
36 which is very similar to PARAREAL, the diagonalization technique [38] (50 citat. since
37 2008), *Revisionist Integral Deferred Corrections* (RIDC) [6] (108 citat. since 2010),

*Submitted to the editors DATE.

Funding: This project has received funding from the European High-Performance Computing Joint Undertaking (JU) under grant agreement No 955701. The JU receives support from the European Union's Horizon 2020 research and innovation programme and Belgium, France, Germany, and Switzerland. This project also received funding from the German Federal Ministry of Education and Research (BMBF) grant 16HPC048.

[†]University of Geneva, Switzerland.

[‡]Hamburg University of Technology, Germany (thibaut.lunet@tuhh.de).

[§]Forschungszentrum Jülich GmbH, Germany.

¹See also <https://www.parallel-in-time.org>

²Number of citations since publication, according to Google Scholar in July 2022.

38 PARAREXP [20] (89 citat. since 2013) or *parallel Rational approximation of EXponential*
 39 *Integrators* (REXI) [46] (23 citat. since 2018).

40 PARAREAL, PFASST, MGRIT and STMG have all been benchmarked for large-
 41 scale problems using large numbers of cores of high-performance computing sys-
 42 tems [33, 35, 37, 48]. They cast the solution process in time as a large linear
 43 or nonlinear system which is solved by iterating on all time steps simultaneously.
 44 Since parallel performance is strongly linked to the rate of convergence, understand-
 45 ing convergence mechanisms and obtaining reliable error bounds for these iterative
 46 PinT methods is crucial. Individual analyses exist for PARAREAL [2, 21, 26, 43, 49],
 47 MGRIT [8, 32, 47], PFASST [3, 4], and STMG [25]. There are also a few combined
 48 analyses showing equivalences between PARAREAL and MGRIT [14, 22] or connec-
 49 tions between MGRIT and PFASST [39]. However, no systematic comparison of
 50 convergence behaviour, let alone efficiencies, between these methods exists.

51 There are at least three obstacles to comparing these four methods: first, there
 52 is no common formalism or notation to describe them; second, the existing analy-
 53 ses use very different techniques to obtain convergence bounds; third, the algorithms
 54 can be applied to many different problems in different ways with many tunable pa-
 55 rameters, all of which affect performance [28]. Our main contribution is to address,
 56 at least for the Dahlquist test problem, the first two problems by proposing a com-
 57 mon formalism to rigorously describe PARAREAL, PFASST, MGRIT³ and the Time
 58 Multi-Grid (TMG) component⁴ of STMG using the same notation. Then, we ob-
 59 tain comparable error bounds for all four methods by using the Generating Function
 60 Method (GFM) [34]. GFM has been used to analyze PARAREAL [21] and was used
 61 to relate PARAREAL and MGRIT [22]. However, our use of GFM to derive common
 62 convergence bounds across multiple algorithms is novel, as is the presented unified
 63 framework. When coupled with a predictive model for computational cost, this GFM
 64 framework could eventually be extended to a model to compare parallel performance
 65 of different algorithms, but this is left for future work.

66 Our manuscript is organized as follows: In Section 2, we introduce the GFM
 67 framework. In particular, in Section 2.1, we give three definitions (time block, block
 68 variable and block operator) used to build the GFM framework and provide some
 69 examples using classical time integration methods. Section 2.2 contains the central
 70 definition of a *block iteration* and again examples. In Section 2.3, we state the main
 71 theoretical results and error bounds, and the next sections contain how existing algo-
 72 rithms from the PinT literature can be expressed in the GFM framework: PARAREAL
 73 in Section 3, TMG in Section 4, and PFASST in Section 5. Finally, we compare in
 74 Section 6 all methods using the GFM framework. Conclusions and an outlook are
 75 given in Section 7.

76 **2. The Generating Function Method.** We consider the Dahlquist equation

$$77 \quad (2.1) \quad \frac{du}{dt} = \lambda u, \quad \lambda \in \mathbb{C}, \quad t \in (0, T], \quad u(0) = u_0 \in \mathbb{C}.$$

78 The complex parameter λ allows us to emulate problems of parabolic ($\lambda < 0$), hyper-
 79 bolic (λ imaginary) and mixed type.

³We do not analyze in detail MGRIT with FCF relaxation, only with F relaxation, in which case the two level variant is equivalent to PARAREAL. Our framework could however be extended to include FCF relaxation, see Remark 3.1.

⁴Since we focus only on the time dimension, the spatial component of STMG is left out.

80 **2.1. Blocks, block variables, and block operators.** We decompose the
 81 time interval $[0, T]$ into N time sub-intervals $[t_n, t_{n+1}]$ of uniform size Δt with $n \in$
 82 $\{0, \dots, N - 1\}$.

83 DEFINITION 2.1 (time block). A time block (or simply block) denotes the dis-
 84 cretization of a time sub-interval $[t_n, t_{n+1}]$ using $M > 0$ grid points,

$$85 \quad (2.2) \quad \tau_{n,m} = t_n + \Delta t \tau_m, \quad m \in \{1, \dots, M\},$$

86 where the $\tau_m \in [0, 1]$ denote normalized grid points in time used for all blocks.

87 We choose the name “block” in order to have a generic name for the internal steps
 88 inside each time sub-interval. A block could be several time steps of a classical time-
 89 stepping scheme (e.g. Runge-Kutta, cf. Section 2.1.1), the quadrature nodes of a
 90 collocation method (cf. Section 2.1.2) or a combination of both. But in every case,
 91 a block represents the time domain that is associated to one computational process
 92 of the time parallelization. A block can also collapse by setting $M := 1$ and $\tau_1 := 1$,
 93 so that we retrieve a standard uniform time-discretization with time step Δt . The
 94 additional structure provided by blocks will be useful when describing and analyzing
 95 two-level methods which use different numbers of grid points per block for each level,
 96 cf. Section 4.2.

97 DEFINITION 2.2 (block variable). A block variable is a vector

$$98 \quad (2.3) \quad \mathbf{u}_n = [u_{n,1}, u_{n,2}, \dots, u_{n,M}]^T,$$

99 where $u_{n,m}$ is an approximation of $u(\tau_{n,m})$ on the time block for the time sub-interval
 100 $[t_n, t_{n+1}]$. For $M = 1$, \mathbf{u}_n reduces to a scalar approximation of $u(\tau_{n,M}) \equiv u(t_{n+1})$.

101 Some iterative PinT methods like PARAREAL (see Section 3) use values defined at
 102 the interfaces between sub-intervals $[t_n, t_{n+1}]$. Other algorithms, like PFASST (see
 103 Section 5), update solution values in the interior of blocks. In the first case, the block
 104 variable is the right interface value with $M = 1$ and thus $\tau_1 = 1$. In the second case,
 105 it consists of *volume* values in the time block $[t_n, t_{n+1}]$ with $M > 1$. In both cases,
 106 PinT algorithms can be defined as *iterative processes updating the block variables*.

107 *Remark 2.3.* While the adjective “time” is natural for evolution problems, PinT
 108 algorithms can also be applied to recurrence relations in different contexts like deep
 109 learning [29] or when computing Gauss quadrature formulas [24]. Therefore, we will
 110 not systematically mention “time” when talking about blocks and block variables.

111 DEFINITION 2.4 (block operators). We denote as block operators the two linear
 112 functions $\phi : \mathbb{C}^M \rightarrow \mathbb{C}^M$ and $\chi : \mathbb{C}^M \rightarrow \mathbb{C}^M$ for which the block variables of a
 113 numerical solution of (2.1) satisfy

$$114 \quad (2.4) \quad \phi(\mathbf{u}_1) = \chi(u_0 \mathbf{I}), \quad \phi(\mathbf{u}_{n+1}) = \chi(\mathbf{u}_n), \quad n = 1, 2, \dots, N - 1,$$

115 with $\mathbf{I} := [1, \dots, 1]^T$. The time integration operator ϕ is bijective and χ is a trans-
 116 mission operator. The time propagator updating \mathbf{u}_n to \mathbf{u}_{n+1} is given by

$$117 \quad (2.5) \quad \psi := \phi^{-1} \chi.$$

118 **2.1.1. Example with Runge-Kutta methods.** Consider numerical integra-
 119 tion of (2.1) with a Runge-Kutta method with stability function

$$120 \quad (2.6) \quad R(z) \approx e^z.$$

121 Using ℓ equidistant time steps per block, there are two natural ways to write the
 122 method using block operators:

123 1. *The volume formulation:* set $M := \ell$ with $\tau_m := m/M$, $m = 1, \dots, M$.
 124 Setting $r := R(\lambda\Delta t/\ell)^{-1}$, the block operators are the $M \times M$ sparse matrices

$$125 \quad (2.7) \quad \phi := \begin{pmatrix} r & & & \\ -1 & r & & \\ & & \ddots & \\ & & & \ddots \end{pmatrix}, \quad \chi := \begin{pmatrix} 0 & \dots & 0 & 1 \\ \vdots & & \vdots & 0 \\ & & \vdots & \\ \vdots & & \vdots & \vdots \end{pmatrix}.$$

126 2. *The interface formulation:* set $M := 1$ so that

$$127 \quad (2.8) \quad \phi := R(\lambda\Delta t/\ell)^{-\ell}, \quad \chi := 1.$$

128 **2.1.2. Example with collocation methods.** Collocation methods are special
 129 implicit Runge-Kutta methods [51, Chap. IV, Sec. 4] and instrumental when defining
 130 PFASST in Section 5. We show their representation with block operators. Starting
 131 from the Picard formulation for (2.1) in one time sub-interval $[t_n, t_{n+1}]$,

$$132 \quad (2.9) \quad u(t) = u(t_n) + \int_{t_n}^t \lambda u(\tau) d\tau,$$

133 we choose a quadrature rule to approximate the integral. We consider only Lobatto
 134 or Radau-II type quadrature nodes where the last quadrature node coincides with
 135 the right sub-interval boundary. This gives us quadrature nodes for each sub-interval
 136 that form the block discretization points $\tau_{n,m}$ of Definition 2.1, with $\tau_M = 1$. We
 137 approximate the solution $u(\tau_{n,m})$ at each node by

$$138 \quad (2.10) \quad u_{n,m} = u_{n,0} + \lambda\Delta t \sum_{j=1}^M q_{m,j} u_{n,j} \quad \text{with} \quad q_{m,j} := \int_0^{\tau_m} l_j(s) ds,$$

139 where l_j are the Lagrange polynomials associated with the nodes τ_m . Combining all
 140 the nodal values, we form the block variable \mathbf{u}_n , which satisfies the linear system

$$141 \quad (2.11) \quad (\mathbf{I} - \mathbf{Q})\mathbf{u}_n = \begin{pmatrix} u_{n,0} \\ \vdots \\ u_{n,0} \end{pmatrix} = \begin{bmatrix} 0 & \dots & 0 & 1 \\ \vdots & & \vdots & \\ 0 & \dots & 0 & 1 \end{bmatrix} \mathbf{u}_{n-1} =: \mathbf{H}\mathbf{u}_{n-1},$$

142 with the quadrature matrix $\mathbf{Q} := \lambda\Delta t(q_{m,j})$, \mathbf{I} the identity matrix, and \mathbf{H} sometimes
 143 called the transfer matrix that copies the last value of the previous time block to
 144 obtain the initial value $u_{n,0}$ of the current block⁵. The integration and transfer block
 145 operators from Definition 2.4 then become⁶ $\phi := (\mathbf{I} - \mathbf{Q})$, $\chi := \mathbf{H}$.

146 **2.2. Block iteration.** Having defined the block operators for our problem, we
 147 write the numerical approximation (2.4) of (2.1) as the *all-at-once global problem*

$$148 \quad (2.12) \quad \mathbf{A}\mathbf{u} := \begin{pmatrix} \phi & & & \\ -\chi & \phi & & \\ & & \ddots & \\ & & & -\chi & \phi \end{pmatrix} \begin{bmatrix} \mathbf{u}_1 \\ \mathbf{u}_2 \\ \vdots \\ \mathbf{u}_N \end{bmatrix} = \begin{bmatrix} \chi(u_0\mathbf{I}) \\ 0 \\ \vdots \\ 0 \end{bmatrix} =: \mathbf{f}.$$

⁵This specific form of the matrix \mathbf{H} comes from the use of Lobatto or Radau-II rules, which treat the right interface of the time sub-interval as a node. A similar description can also be obtained for Radau-I or Gauss-type quadrature rules that do not use the right boundary as node, but we omit it for the sake of simplicity.

⁶The notation \mathbf{H} is specific to SDC and collocation methods (see *e.g.* [3]), while the χ notation from the GFM framework is generic for arbitrary time integration methods.

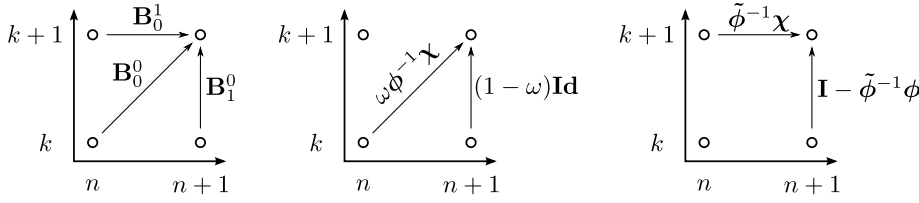


FIG. 1. kn -graphs for a generic Primary Block Iteration (left), damped Block Jacobi (middle) and Approximate Block Gauss-Seidel (right).

149 Iterative PinT algorithms solve (2.12) by updating a vector $\mathbf{u}^k = [\mathbf{u}_1^k, \dots, \mathbf{u}_N^k]^T$ to
 150 \mathbf{u}^{k+1} until some stopping criterion is satisfied. If the global iteration can be written
 151 as a local update for each block variable separately, we call the local update formula
 152 a *block iteration*.

153 **DEFINITION 2.5** (Primary block iteration). A primary block iteration is an up-
 154 dating formula for $n \geq 0$ of the form

$$155 \quad (2.13) \quad \mathbf{u}_{n+1}^{k+1} = \mathbf{B}_{n+1}^0(\mathbf{u}_{n+1}^k) + \mathbf{B}_0^1(\mathbf{u}_n^{k+1}) + \mathbf{B}_0^0(\mathbf{u}_n^k), \quad \mathbf{u}_0^k = u_0 \mathbf{I} \quad \forall k \in \mathbb{N},$$

156 where \mathbf{B}_1^0 , \mathbf{B}_0^1 and \mathbf{B}_0^0 are linear operators from \mathbb{C}^M to \mathbb{C}^M that satisfy the consistency
 157 condition⁷

$$158 \quad (2.14) \quad (\mathbf{B}_1^0 - \mathbf{I})\boldsymbol{\psi} + \mathbf{B}_0^1 + \mathbf{B}_0^0 = 0,$$

159 with $\boldsymbol{\psi}$ defined in (2.5).

160 Note that a block iteration is always associated with an all-at-once global problem,
 161 and the primary block iteration (2.13) should converge to the solution of (2.12).

162 Figure 1 (left) shows a graphical representation of a primary block iteration using
 163 a kn -graph to represent the dependencies of \mathbf{u}_{n+1}^{k+1} on the other block variables. The
 164 x -axis represents the block index n (time), and the y -axis represents the iteration
 165 index k . Arrows show dependencies from previous n or k indices and can only go
 166 from left to right and/or from bottom to top. For the primary block iteration, we
 167 consider only dependencies from the previous block n and iterate k for \mathbf{u}_{n+1}^{k+1} .

168 More general block iterations can also be considered for specific iterative PinT
 169 methods, e.g. MGRIT with FCF-relaxation (see Remark 3.1). Other algorithms
 170 also consist of combinations of two or more block iterations, for example STMG
 171 (cf. Section 4) or PFASST (cf. Section 5). But we show in those sections that we
 172 can reduce those combinations into a single primary block iteration, hence we focus
 173 here mostly on primary block iterations to introduce our analysis framework.

174 We next describe the Block Jacobi relaxation (Section 2.2.1) and the Approximate
 175 Block Gauss-Seidel iteration (Section 2.2.2), which are key components used to
 176 describe iterative PinT methods.

177 **2.2.1. Block Jacobi relaxation.** A damped block Jacobi iteration for the
 178 global problem (2.12) can be written as

$$179 \quad (2.15) \quad \mathbf{u}^{k+1} = \mathbf{u}^k + \omega \mathbf{D}^{-1}(\mathbf{f} - \mathbf{A}\mathbf{u}^k),$$

⁷ Condition (2.14) is necessary for the block iteration to have the correct fixed point.

180 where \mathbf{D} is a block diagonal matrix constructed with the integration operator ϕ , and
 181 $\omega > 0$ is a relaxation parameter. For $n > 0$, the corresponding block formulation is

$$182 \quad (2.16) \quad \mathbf{u}_{n+1}^{k+1} = (1 - \omega)\mathbf{u}_{n+1}^k + \omega\phi^{-1}\chi\mathbf{u}_n^k,$$

183 which is a primary block iteration with $\mathbf{B}_0^1 = 0$. Its kn -graph is shown in Figure 1
 184 (middle). The consistency condition (2.14) is satisfied, since

$$185 \quad (2.17) \quad ((1 - \omega)\mathbf{I} - \mathbf{I})\phi^{-1}\chi + 0 + \omega\phi^{-1}\chi = 0.$$

186 Note that selecting $\omega = 1$ simplifies the block iteration to

$$187 \quad (2.18) \quad \mathbf{u}_{n+1}^{k+1} = \phi^{-1}\chi\mathbf{u}_n^k.$$

188 **2.2.2. Approximate Block Gauss-Seidel iteration.** Let us consider a Block
 189 Gauss-Seidel type preconditioned iteration for the global problem (2.12),

$$190 \quad (2.19) \quad \mathbf{u}^{k+1} = \mathbf{u}^k + \mathbf{P}_{GS}^{-1}(\mathbf{f} - \mathbf{A}\mathbf{u}^k), \quad \mathbf{P}_{GS} = \begin{bmatrix} \tilde{\phi} & & & \\ -\chi & \tilde{\phi} & & \\ & \ddots & \ddots & \\ & & & \end{bmatrix},$$

191 where the block operator $\tilde{\phi}$ corresponds to an approximation of ϕ . This approximation
 192 can be based on time-step coarsening, but could also use other approaches, *e.g.* a
 193 lower-order time integration method. In general, $\tilde{\phi}$ must be cheaper than ϕ , but is
 194 also less accurate. Subtracting \mathbf{u}^k in (2.19) and multiplying by \mathbf{P}_{GS} yields the block
 195 iteration of this *Approximate Block Gauss-Seidel* (ABGS),

$$196 \quad (2.20) \quad \mathbf{u}_{n+1}^{k+1} = [\mathbf{I} - \tilde{\phi}^{-1}\phi] \mathbf{u}_{n+1}^k + \tilde{\phi}^{-1}\chi\mathbf{u}_n^{k+1}.$$

197 Its kn -graph is shown in Figure 1 (right). Note that a standard block Gauss-Seidel
 198 iteration for (2.12) (*i.e.* with $\tilde{\phi} = \phi$) is actually a direct solver, the iteration converges
 199 in one step by integrating all blocks with ϕ sequentially, and its block iteration is
 200 simply

$$201 \quad (2.21) \quad \mathbf{u}_{n+1}^{k+1} = \phi^{-1}\chi\mathbf{u}_n^{k+1}.$$

202 **2.3. Generating function and error bound for a block iteration.** Before
 203 giving a generic expression for the error bound of the primary block iteration (2.13)
 204 using the GFM framework, we first need a definition and a preliminary result. The
 205 primary block iteration (2.13) is defined for each block index $n \geq 0$, thus we can define

206 **DEFINITION 2.6** (Generating function). *The generating function associated with*
 207 *the primary block iteration (2.13) is the power series*

$$208 \quad (2.22) \quad \rho_k(\zeta) := \sum_{n=0}^{\infty} e_{n+1}^k \zeta^{n+1},$$

209 where $e_{n+1}^k := \|\mathbf{u}_{n+1}^k - \mathbf{u}_{n+1}\|$ is the difference between the k^{th} iterate \mathbf{u}_{n+1}^k and the
 210 exact solution \mathbf{u}_{n+1} for one block of (2.4) in some norm on \mathbb{C}^M .

211 Since the analysis works in any norm, we do not specify a particular one here. In the
 212 numerical examples we use the L^∞ norm on \mathbb{C}^M .

213 LEMMA 2.7. *The generating function for the primary block iteration (2.13) satis-*
 214 *fies*

$$215 \quad (2.23) \quad \rho_{k+1}(\zeta) \leq \frac{\gamma + \alpha\zeta}{1 - \beta\zeta} \rho_k(\zeta),$$

216 where $\alpha := \|\mathbf{B}_0^0\|$, $\beta := \|\mathbf{B}_0^1\|$, $\gamma := \|\mathbf{B}_1^0\|$, and the operator norm is induced by the
 217 chosen vector norm.

218 *Proof.* We start from (2.13) and subtract the exact solution of (2.4),

$$219 \quad (2.24) \quad \mathbf{u}_{n+1}^{k+1} - \mathbf{u}_{n+1} = \mathbf{B}_1^0(\mathbf{u}_{n+1}^k) + \mathbf{B}_0^1(\mathbf{u}_n^{k+1}) + \mathbf{B}_0^0(\mathbf{u}_n^k) - \psi(\mathbf{u}_n).$$

220 Using the linearity of the block operators and (2.14) with \mathbf{u}_n , this simplifies to

$$221 \quad (2.25) \quad \mathbf{u}_{n+1}^{k+1} - \mathbf{u}_{n+1} = \mathbf{B}_1^0(\mathbf{u}_{n+1}^k - \mathbf{u}_{n+1}) + \mathbf{B}_0^1(\mathbf{u}_n^{k+1} - \mathbf{u}_n) + \mathbf{B}_0^0(\mathbf{u}_n^k - \mathbf{u}_n).$$

222 We apply the norm, use the triangle inequality and the operator norms defined above
 223 to get the recurrence relation

$$224 \quad (2.26) \quad e_{n+1}^{k+1} \leq \gamma e_{n+1}^k + \beta e_n^{k+1} + \alpha e_n^k$$

225 for the error. We multiply this inequality by ζ^{n+1} and sum for $n \in \mathbb{N}$ to get

$$226 \quad (2.27) \quad \sum_{n=0}^{\infty} e_{n+1}^{k+1} \zeta^{n+1} \leq \gamma \sum_{n=0}^{\infty} e_{n+1}^k \zeta^{n+1} + \beta \sum_{n=0}^{\infty} e_n^{k+1} \zeta^{n+1} + \alpha \sum_{n=0}^{\infty} e_n^k \zeta^{n+1}.$$

227 Note that this is a formal power series expansion for ζ small in the sense of generating
 228 functions [34, Section 1.2.9]. Using Definition 2.6 and that $e_0^k = 0$ for all k we find

$$229 \quad (2.28) \quad \rho_{k+1}(\zeta) \leq \gamma \rho_k(\zeta) + \beta \zeta \sum_{n=1}^{\infty} e_n^{k+1} \zeta^n + \alpha \zeta \sum_{n=1}^{\infty} e_n^k \zeta^n.$$

230 Shifting indices leads to

$$231 \quad (2.29) \quad (1 - \beta\zeta) \rho_{k+1}(\zeta) \leq (\gamma + \alpha\zeta) \rho_k(\zeta)$$

232 and concludes the proof. \square

233 THEOREM 2.8. *Consider the primary block iteration (2.13) and let*

$$234 \quad (2.30) \quad \delta := \max_{n=1, \dots, N} \|\mathbf{u}_n^0 - \mathbf{u}_n\|$$

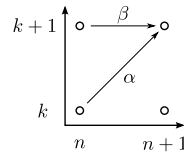
235 *be the maximum error of the initial guess over all blocks. Then, using the notation of*
 236 *Lemma 2.7, we have*

$$237 \quad (2.31) \quad e_{n+1}^k \leq \theta_{n+1}^k(\alpha, \beta, \gamma) \delta$$

238 *for $k > 0$, where θ_{n+1}^k is a bounding function defined as follows:*

- 239 • *if only $\gamma = 0$, then*

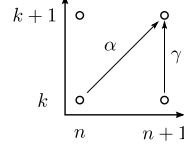
$$240 \quad (2.32) \quad \theta_{n+1}^k = \frac{\alpha^k}{(k-1)!} \sum_{i=0}^{n-k} \prod_{l=1}^{k-1} (i+l) \beta^i;$$



241

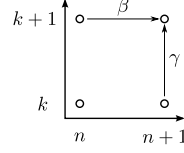
- if only $\beta = 0$, then

$$(2.33) \quad \theta_{n+1}^k = \begin{cases} (\gamma + \alpha)^k & \text{if } k \leq n, \\ \gamma^k \sum_{i=0}^n \binom{k}{i} \left(\frac{\alpha}{\gamma}\right)^i & \text{otherwise;} \end{cases}$$



- if only $\alpha = 0$, then

$$(2.34) \quad \theta_{n+1}^k = \frac{\gamma^k}{(k-1)!} \sum_{i=0}^n \prod_{l=1}^{k-1} (i+l) \beta^i;$$



- if neither α , nor β , nor γ are zero, then

$$(2.35) \quad \theta_{n+1}^k = \gamma^k \sum_{i=0}^{\min(n,k)} \sum_{l=0}^{n-i} \binom{k}{i} \binom{l+k-1}{l} \left(\frac{\alpha}{\gamma}\right)^i \beta^l.$$

We call any error bound obtained from one of these formulas a GFM-bound.

The proof uses Lemma 2.7 to bound the generating function at $k = 0$ by

$$(2.36) \quad \rho_0(\zeta) \leq \delta \sum_{n=0}^{\infty} \zeta^{n+1},$$

which covers arbitrary initial guesses for defining starting values \mathbf{u}_n^0 for each block. For specific initial guesses, $\rho_0(\zeta)$ can be bounded differently [21, Proof of Th. 1]. The error bound is then computed by coefficient identification after a power series expansion. The rather technical proof can be found in Appendix A.

In the numerical examples shown below, we find that the estimate from Theorem 2.8 is not always sharp, cf. Section 5.5.1. If the last time point of the blocks coincides with the right bound of the sub-interval⁸, it is helpful to define the *interface error* at the right boundary point of the n^{th} block as

$$(2.37) \quad \bar{e}_{n+1}^k := |\bar{u}_{n+1}^k - \bar{u}_n^k|,$$

where \bar{u} is the last element of the block variable \mathbf{u} . We then multiply (2.25) by $\mathbf{e}_M^T = [0, \dots, 0, 1]$ to get

$$(2.38) \quad \mathbf{e}_M^T (\mathbf{u}_{n+1}^{k+1} - \mathbf{u}_{n+1}^k) = \mathbf{b}_1^0 (\mathbf{u}_{n+1}^k - \mathbf{u}_{n+1}^k) + \mathbf{b}_0^1 (\mathbf{u}_n^{k+1} - \mathbf{u}_n^k) + \mathbf{b}_0^0 (\mathbf{u}_n^k - \mathbf{u}_n^k),$$

where \mathbf{b}_i^j is the last row of the block operator \mathbf{B}_i^j . Taking the absolute value on both sides, we recognize the interface error \bar{e}_{n+1}^{k+1} on the left hand side. By neglecting the error from interior points and using the triangle inequality, we get the approximation⁹

$$(2.39) \quad \bar{e}_{n+1}^{k+1} \lesssim \bar{\gamma} \bar{e}_{n+1}^k + \bar{\beta} \bar{e}_n^{k+1} + \bar{\alpha} \bar{e}_n^k,$$

where $\bar{\alpha} := |\bar{b}_0^0|$, $\bar{\beta} := |\bar{b}_1^0|$, $\bar{\gamma} := |\bar{b}_0^1|$.

⁸This is the case for all time-integration methods considered in this paper, even if this is not a necessary condition to use the GFM framework.

⁹For an interface block iteration ($M = 1, \tau_1 = 1$), (2.39) becomes a rigorous inequality and Corollary 2.9 thus becomes an upper bound.

270 COROLLARY 2.9 (Interface error approximation). *Defining for the initial inter-*
 271 *face error the bound $\bar{\delta} := \max_{n \in \{1, \dots, N\}} \|\bar{u}_n^0 - \bar{u}_n\|$, we obtain for the interface error*
 272 *the approximation*

$$273 \quad (2.40) \quad \bar{e}_{n+1}^k \lesssim \bar{\theta}_{n+1}^k \bar{\delta}, \quad \bar{\theta}_{n+1}^k := \theta_{n+1}^k(\bar{\alpha}, \bar{\beta}, \bar{\gamma}),$$

274 with θ_{n+1}^k defined in Theorem 2.8.

275 *Proof.* The result follows as in the proof of Lemma 2.7 using approximate rela-
 276 tions. \square

277 *Remark 2.10.* For the general case, the error at the interface \bar{e}_{n+1}^{k+1} is not the same
 278 as the error for the whole block e_{n+1}^{k+1} . Only a block discretization using a single point
 279 ($M = 1$) makes the two values identical. Furthermore, Corollary 2.9 is generally not
 280 an upper bound, but an approximation thereof.

281 3. Writing Parareal and MGRIT as block iterations.

282 **3.1. Description of the algorithm.** The PARAREAL algorithm introduced by
 283 Lions et al. [36] corresponds to a block iteration update with scalar blocks ($M = 1$),
 284 and its convergence was analyzed in [26, 43]. We propose here a new description
 285 of PARAREAL in the scope of the GFM framework, which states that PARAREAL is
 286 simply a combination of two preconditioned iterations applied to the global problem
 287 (2.12), namely one Block Jacobi relaxation without damping (Section 2.2.1), followed
 288 by an ABGS iteration (Section 2.2.2).

289 We denote by $\mathbf{u}^{k+1/2}$ the intermediate solution after the Block Jacobi step. Using
 290 (2.18) and (2.20), the two successive primary block iteration steps are

$$291 \quad (3.1) \quad \mathbf{u}_{n+1}^{k+1/2} = \phi^{-1} \chi \mathbf{u}_n^k,$$

$$292 \quad (3.2) \quad \mathbf{u}_{n+1}^{k+1} = [\mathbf{I} - \tilde{\phi}^{-1} \phi] \mathbf{u}_{n+1}^{k+1/2} + \tilde{\phi}^{-1} \chi \mathbf{u}_n^{k+1}.$$

294 Combining both yields the primary block iteration

$$295 \quad (3.3) \quad \mathbf{u}_{n+1}^{k+1} = [\phi^{-1} \chi - \tilde{\phi}^{-1} \chi] \mathbf{u}_n^k + \tilde{\phi}^{-1} \chi \mathbf{u}_n^{k+1}.$$

296 Now as stated in Section 2.2.2, $\tilde{\phi}$ is an approximation of the integration operator ϕ ,
 297 that is cheaper to invert but less accurate¹⁰. In other words, if we define

$$298 \quad (3.4) \quad \mathcal{F} := \phi^{-1} \chi, \quad \mathcal{G} := \tilde{\phi}^{-1} \chi,$$

299 to be a fine and coarse propagator on one block, then (3.3) becomes

$$300 \quad (3.5) \quad \mathbf{u}_{n+1}^{k+1} = \mathcal{F} \mathbf{u}_n^k + \mathcal{G} \mathbf{u}_n^{k+1} - \mathcal{G} \mathbf{u}_n^k,$$

301 which is the PARAREAL update formula derived from the approximate Newton update
 302 in the multiple shooting approximation in [26]. Iteration (3.5) is a primary block
 303 iteration in the sense of Definition 2.5 with $\mathbf{B}_1^0 := 0$, $\mathbf{B}_0^1 := \mathcal{G}$ and $\mathbf{B}_0^0 := \mathcal{F} - \mathcal{G}$. Its
 304 kn -graph is shown in Figure 2 (left). The consistency condition (2.14) is satisfied,
 305 since $(0 - \mathbf{I})\mathcal{F} + \mathcal{G} + (\mathcal{F} - \mathcal{G}) = 0$. If we subtract \mathbf{u}_{n+1}^k in (3.3), multiply both sides

¹⁰In the original paper [36], this approximation is done using larger time-steps, but many other types of approximations have been used since then in the literature.

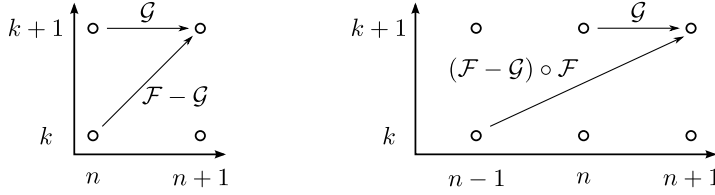


FIG. 2. kn -graphs for PARAREAL/MGRIT with F -relaxation (left) and MGRIT with FCF-relaxation/PARAREAL with overlap (right).

306 by ϕ and rearrange terms, we can write PARAREAL as the preconditioned fixed point
307 iteration

$$308 \quad (3.6) \quad \mathbf{u}^{k+1} = \mathbf{u}^k + \mathbf{M}^{-1}(\mathbf{f} - \mathbf{A}\mathbf{u}^k), \quad \mathbf{M} := \begin{pmatrix} \phi & & & \\ -\phi\tilde{\phi}^{-1}\chi & \phi & & \\ & & \ddots & \\ & & & \ddots \end{pmatrix},$$

309 with iteration matrix $\mathbf{R}_{\text{PARAREAL}} = \mathbf{I} - \mathbf{M}^{-1}\mathbf{A}$.

310 *Remark 3.1.* It is known in the literature that PARAREAL is equivalent to a two-
311 level MGRIT algorithm with F -relaxation [14, 22, 47]. In MGRIT, one however also
312 often uses FCF-relaxation, which is a combination of *two* non-damped ($\omega = 1$) Block
313 Jacobi relaxation steps, followed by an ABGS step: denoting by $\mathbf{u}^{k+1/3}$ and $\mathbf{u}^{k+2/3}$
314 the intermediary block Jacobi iterations, we obtain

$$315 \quad (3.7) \quad \mathbf{u}_{n+1}^{k+1/3} = \phi^{-1}\chi\mathbf{u}_n^k,$$

$$316 \quad (3.8) \quad \mathbf{u}_{n+1}^{k+2/3} = \phi^{-1}\chi\mathbf{u}_n^{k+1/3},$$

$$317 \quad (3.9) \quad \mathbf{u}_{n+1}^{k+1} = [\mathbf{I} - \tilde{\phi}^{-1}\phi]\mathbf{u}_{n+1}^{k+2/3} + \tilde{\phi}^{-1}\chi\mathbf{u}_n^{k+1}.$$

319 Shifting the n index in the first Block Jacobi iteration, combining all of them and
320 re-using the \mathcal{F} and \mathcal{G} notation then gives

$$321 \quad (3.10) \quad \mathbf{u}_{n+1}^{k+1} = \mathbf{B}_{-1}^0(\mathbf{u}_{n-1}^k) + \mathbf{B}_0^1(\mathbf{u}_n^{k+1}), \quad \mathbf{B}_{-1}^0 = (\mathcal{F} - \mathcal{G})\mathcal{F}, \quad \mathbf{B}_0^1 = \mathcal{G},$$

322 which is the update formula of PARAREAL with overlap, shown to be equivalent to
323 MGRIT with FCF-relaxation [22, Th. 4]¹¹.

324 This block iteration, whose kn -graph is represented in Figure 2 (right), does not
325 only link two successive block variables with time index $n + 1$ and n , but also uses
326 a block with time index $n - 1$. It is not a primary block iteration in the sense of
327 Definition 2.5 anymore. Although it can be analyzed using generating functions [22,
328 Th. 6], we focus on primary block iterations here and leave more complex block
329 iterations like this one for future work.

330 **3.2. Convergence analysis with GFM bounds.** In their convergence analy-
331 sis of PARAREAL for non-linear problems [21], the authors obtain a double recurrence
332 of the form $e_{n+1}^{k+1} \leq \alpha e_n^k + \beta e_n^{k+1}$, where α and β come from Lipschitz constants

¹¹It was shown in [22] that MGRIT with (FC) $^\nu$ F-relaxation, where $\nu > 0$ is the number of additional FC-relaxations, is equivalent to an overlapping version of PARAREAL with ν overlaps. Generalizing our computations shows that those algorithms are equivalent to $(\nu - 1)$ non-damped Block Jacobi iterations followed by an ABGS step.

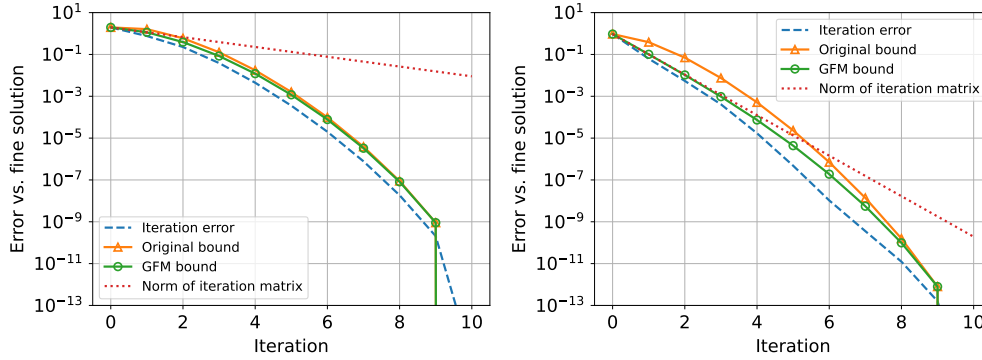


FIG. 3. Error bounds for PARAREAL for (2.1). Left: $\lambda = i$, right: $\lambda = -1$. Note that for $\lambda = i$, the GFM-bound and the original one are almost identical.

333 and local truncation error bounds. Using the same notation as in Section 3.1, with
 334 $\alpha = \|\mathcal{F} - \mathcal{G}\|$ and $\beta = \|\mathcal{G}\|$, we find [21, Th. 1] that

$$335 \quad (3.11) \quad e_{n+1}^k \leq \delta \frac{\alpha^k}{k!} \bar{\beta}^{n-k} \prod_{l=1}^k (n+1-l), \quad \bar{\beta} = \max(1, \beta).$$

336 This is different from the GFM bound

$$337 \quad (3.12) \quad e_{n+1}^k \leq \delta \frac{\alpha^k}{(k-1)!} \sum_{i=0}^{n-k} \prod_{l=1}^{k-1} (i+l) \beta^i$$

338 we get when applying Theorem 2.8 with $\gamma = 0$ to the block iteration of PARAREAL.
 339 The difference stems from an approximation in the proof of [21, Th. 1] which leads
 340 to the simpler and more explicit bound in (3.11). The two bounds are equal when
 341 $\beta = 1$, but for $\beta \neq 1$, the GFM bound in (3.12) is sharper. To illustrate this, we use
 342 the interface formulation of Section 2.1.1: we set $M := 1$, $\tau_1 := 1$ and use the block
 343 operators

$$344 \quad (3.13) \quad \phi := R(\lambda \Delta t / \ell)^{-\ell}, \quad \chi := 1, \quad \tilde{\phi} := R_{\Delta}(\lambda \Delta t / \ell_{\Delta})^{-\ell_{\Delta}}.$$

345 We solve (2.1) for $\lambda \in \{i, -1\}$ with $t \in [0, 2\pi]$ and $u_0 = 1$, using $N := 10$ blocks,
 346 $\ell := 10$ fine time steps per block, the standard 4th-order Runge-Kutta method for ϕ
 347 and $\ell_{\Delta} = 5$ coarse time steps per block with Backward Euler for $\tilde{\phi}$. Figure 3 shows
 348 the resulting error (dashed line) at the last time point, the original error bound (3.11),
 349 and the new bound (3.12). We also plot the linear bound obtained from the L^{∞} norm
 350 of the iteration matrix $\mathbf{R}_{\text{PARAREAL}}$ defined just after (3.6). For both values of λ , the
 351 GFM-bounds coincide with the linear bound from $\mathbf{R}_{\text{PARAREAL}}$ for the first iteration,
 352 and the GFM-bound captures the super-linear contraction in later iterations. For
 353 $\lambda = i$, the old and new bounds are similar since β is close to 1. However, for $\lambda = -1$
 354 where β is smaller than one, the new bound gives a sharper estimate of the error,
 355 and we can also see that the new bound captures well the transition from the linear
 356 to the super-linear convergence regime. On the left in Figure 3, PARAREAL seems to
 357 converge well for imaginary $\lambda = i$. This, however, should not be seen as a working
 358 example of PARAREAL for a hyperbolic type problem, but is rather the effect of the
 359 relatively good accuracy of the coarse solver using 50 points per wave length for one

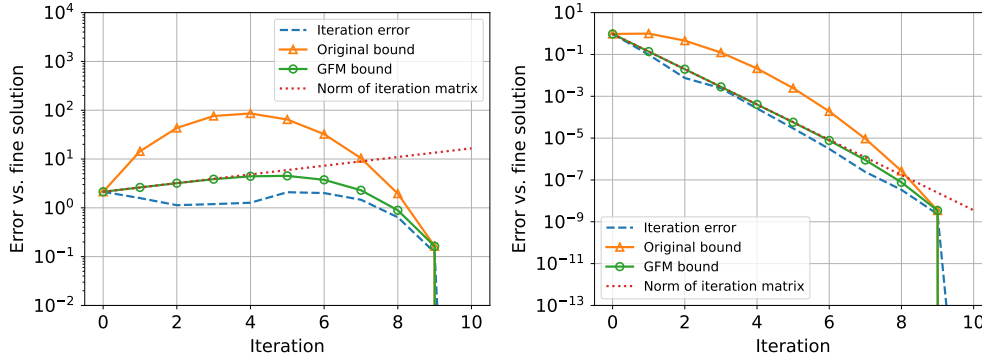


FIG. 4. Error bounds for PARAREAL for (2.1). Left: $\lambda = 4i$, right: $\lambda = -4$.

360 wavelength present in the solution time interval we consider. Denoting by ϵ_Δ the
 361 L_∞ error with respect to the exact solution, the accuracy of the coarse solver ($\epsilon_\Delta =$
 362 $6.22e-01$) allows the PARAREAL error to reach the fine solver error ($\epsilon_\Delta = 8.16e-07$) in
 363 $K = 8$ iterations. Since the ideal parallel speedup of PARAREAL, neglecting the coarse
 364 solver cost, is bounded by $N/K = 1.25$ [1, Sec. 4], this indicates however almost no
 365 speedup in practical applications (see also [28]). If we increase the coarse solver error,
 366 for instance by multiplying λ by a factor 4 to have now four times more wavelength
 367 in the domain, and only 12.5 points per wavelength resolution in the coarse solver,
 368 the convergence of PARAREAL deteriorates massively, as we can see in Figure 4 (left),
 369 while this is not the case for the purely negative real fourfold $\lambda = -4$.

370 This illustrates how Parareal has great convergence difficulties for hyperbolic
 371 problems, already well-documented in the literature see *e.g.* [17, 23]. This is analogous
 372 to the difficulties due to the pollution error and damping in multi-grid methods when
 373 solving medium to high frequency associated time harmonic problems, see [10, 12, 13,
 374 19, 7] and references therein.

375 **4. Writing two-level Time Multi-Grid as a block iteration.** The idea of
 376 time multi-grid (TMG) goes back to the 1980s and 1990s [5, 30, 40]. Furthermore,
 377 not long after PARAREAL was introduced, it was shown to be equivalent to a time
 378 multi-grid method, independently of the type of approximation used for the coarse
 379 solver [26]. This inspired the development of other time multi-level methods, in particu-
 380 lar MGRIT [14]. However, PARAREAL and MGRIT are usually viewed as iterations
 381 acting on values located at the block interface, while TMG-based algorithms, in particu-
 382 lar STMG [25], use an iteration updating volume values (*i.e.* all fine time points
 383 in the time domain). In this section, we focus on a generic description of TMG, and
 384 show how to write its two-level form applied to the Dahlquist problem as block iteration.
 385 In particular, we will show in Section 5 that PFASST can be expressed as a
 386 specific variant of TMG. The extension of this analysis to more levels and comparison
 387 with multi-level MGRIT is left for future work.

388 **4.1. Definition of a coarse block problem for Time Multi-Grid.** To build
 389 a coarse problem, we consider a coarsened version of the global problem (2.12), with a
 390 \mathbf{A}_C matrix having $N \cdot M_C$ rows instead of $N \cdot M$ for \mathbf{A} . For each of the N blocks, let
 391 $(\tau_m^C)_{1 \leq m \leq M_C}$ be the normalized M_C grid points¹² of a *coarser* block discretization,

¹²Those do not need to be a subset of the fine block grid points, although they usually are in applications.

392 with $M_C < M$.

393 We can define a coarse block operator ϕ_C by using the same time integration
 394 method as for ϕ on every block, but with fewer time points. This is equivalent to
 395 geometric coarsening used for h -multigrid (or geometric multigrid [50]), *e.g.* when
 396 using one time-step of a Runge-Kutta method between each time grid point. It can
 397 also be equivalent to spectral coarsening used for p -multigrid (or spectral element
 398 multigrid [42]), *e.g.* when one step of a collocation method on M points is used within
 399 each block (as for PFASST, see Section 5.3).

400 We also consider the associated transmission operator χ_C , and denote by \mathbf{u}_n^C the
 401 block variable on this coarse time block, which satisfies

$$402 \quad (4.1) \quad \phi_C(\mathbf{u}_1^C) = \chi_C \mathbf{T}_F^C(u_0 \mathbf{1}), \quad \phi_C \mathbf{u}_{n+1}^C = \chi_C \mathbf{u}_n^C \quad n = 1, 2, \dots, N-1.$$

403 Let \mathbf{u}^C be the global coarse variable that solves

$$404 \quad (4.2) \quad \mathbf{A}_C \mathbf{u}^C := \begin{pmatrix} \phi_C & & & & \\ -\chi_C & \phi_C & & & \\ & & \ddots & & \\ & & & -\chi_C & \phi_C \end{pmatrix} \begin{bmatrix} \mathbf{u}_1^C \\ \mathbf{u}_2^C \\ \vdots \\ \mathbf{u}_N^C \end{bmatrix} = \begin{bmatrix} \chi_C \mathbf{T}_F^C(u_0 \mathbf{1}) \\ 0 \\ \vdots \\ 0 \end{bmatrix} =: \mathbf{f}^C.$$

405 \mathbf{T}_F^C is a block restriction operator, i.e. a transfer matrix from a fine (F) to a coarse
 406 (C) block discretization. Similarly, we have a block prolongation operator \mathbf{T}_C^F , i.e. a
 407 transfer matrix from a coarse (C) to a fine (F) block discretization.

408 *Remark 4.1.* While both ϕ_C and $\tilde{\phi}$ are approximations of the fine operator ϕ ,
 409 the main difference between ϕ_C and $\tilde{\phi}$ is the size of the vectors they can be applied
 410 to (M_C and M). Furthermore, ϕ_C itself does need the transfer operators \mathbf{T}_C^F and
 411 \mathbf{T}_F^C to compute approximate values on the fine time points, while $\tilde{\phi}$ alone is sufficient
 412 (even if it can hide some restriction and interpolation process within). However, the
 413 definition of a coarse grid correction in the classical multi-grid formalism needs this
 414 separation between transfer and coarse operators (see [50, Sec. 2.2.2]), which limits
 415 the use of $\tilde{\phi}$ and requires the introduction of ϕ_C .

416 **4.2. Block iteration of a Coarse Grid Correction.** Let us consider a stand-
 417 alone Coarse Grid Correction (CGC), without pre- or post-smoothing¹³, of a two-level
 418 multi-grid iteration [31] applied to (2.12). One CGC step applied to (2.12) can be
 419 written as

$$420 \quad (4.3) \quad \mathbf{u}^{k+1} = \mathbf{u}^k + \bar{\mathbf{T}}_C^F \mathbf{A}_C^{-1} \bar{\mathbf{T}}_F^C (\mathbf{f} - \mathbf{A} \mathbf{u}^k),$$

421 where $\bar{\mathbf{T}}_C^F$ denotes the block diagonal matrix formed with \mathbf{T}_C^F on the diagonal, and
 422 similarly for $\bar{\mathbf{T}}_F^C$. When splitting (4.3) into two steps,

$$423 \quad (4.4) \quad \mathbf{A}_C \mathbf{d} = \bar{\mathbf{T}}_F^C (\mathbf{f} - \mathbf{A} \mathbf{u}^k),$$

$$424 \quad (4.5) \quad \mathbf{u}^{k+1} = \mathbf{u}^k + \bar{\mathbf{T}}_C^F \mathbf{d},$$

426 the CGC term (or defect) \mathbf{d} appears explicitly. Expanding the two steps for $n > 0$
 427 into a block formulation and inverting ϕ_C leads to

$$428 \quad (4.6) \quad \mathbf{d}_{n+1} = \phi_C^{-1} \mathbf{T}_F^C \chi \mathbf{u}_n^k - \phi_C^{-1} \mathbf{T}_F^C \phi \mathbf{u}_{n+1}^k + \phi_C^{-1} \chi_C \mathbf{d}_n,$$

$$429 \quad (4.7) \quad \mathbf{u}_{n+1}^{k+1} = \mathbf{u}_{n+1}^k + \mathbf{T}_C^F \mathbf{d}_{n+1}.$$

431 Now we need the following simplifying assumption.

¹³The CGC is not convergent by itself without a smoother.

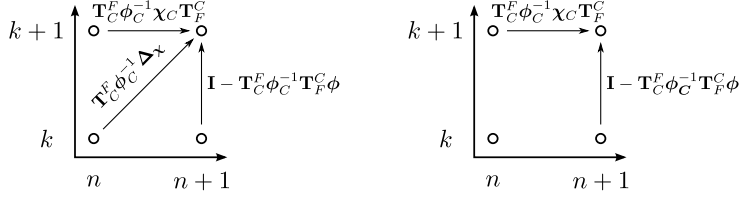


FIG. 5. kn -graphs for the CGC block iteration, with Assumption 4.2 only (left), and with both Assumptions 4.2 and 4.3 (right).

432 Assumption 4.2. Prolongation \mathbf{T}_C^F followed by restriction \mathbf{T}_F^C leaves the coarse
433 block variables unchanged, *i.e.*

$$434 \quad (4.8) \quad \mathbf{T}_F^C \mathbf{T}_C^F = \mathbf{I}.$$

435 This condition is satisfied in many situations (*e.g.* restriction with standard injection
436 on a coarse subset of the fine points, or polynomial interpolation with any possible
437 coarse block discretization)¹⁴. Using it in (4.7) for block index n yields

$$438 \quad (4.9) \quad \mathbf{d}_n = \mathbf{T}_F^C (\mathbf{u}_n^{k+1} - \mathbf{u}_n^k).$$

439 Inserting \mathbf{d}_n into (4.6) on the right and the resulting \mathbf{d}_{n+1} into (4.7) leads to

$$440 \quad (4.10) \quad \mathbf{u}_{n+1}^{k+1} = (\mathbf{I} - \mathbf{T}_C^F \phi_C^{-1} \mathbf{T}_F^C \phi) \mathbf{u}_{n+1}^k + \mathbf{T}_C^F \phi_C^{-1} \chi_C \mathbf{T}_F^C \mathbf{u}_n^{k+1} + \mathbf{T}_C^F \phi_C^{-1} \Delta_\chi \mathbf{u}_n^k,$$

441 with $\Delta_\chi := \mathbf{T}_F^C \chi - \chi_C \mathbf{T}_F^C$. This is a primary block iteration in the sense of Defini-
442 tion 2.5, and we give its kn -graph in Figure 5 (left). We can simplify it further using
443 a second assumption:

444 Assumption 4.3. We consider operators \mathbf{T}_F^C , χ and χ_C such that

$$445 \quad (4.11) \quad \Delta_\chi = \mathbf{T}_F^C \chi - \chi_C \mathbf{T}_F^C = 0.$$

446 This holds for classical time-stepping methods when both left and right time sub-
447 interval boundaries are included in the block variables, or for collocation methods
448 using Radau-II or Lobatto type nodes.

449 This last assumption is important to define PFASST (*cf.* Section 5.3 and see Bolten
450 et al. [3, Remark 1] for more details) and simplifies the analysis of TMG, as both
451 methods use this block iteration. Then, (4.10) reduces to

$$452 \quad (4.12) \quad \mathbf{u}_{n+1}^{k+1} = (\mathbf{I} - \mathbf{T}_C^F \phi_C^{-1} \mathbf{T}_F^C \phi) \mathbf{u}_{n+1}^k + \mathbf{T}_C^F \phi_C^{-1} \mathbf{T}_F^C \chi \mathbf{u}_n^{k+1}.$$

453 Again, this is a primary block iteration for which the kn -graph is given in Figure 5
454 (right). It satisfies the consistency condition¹⁵ (2.14) since $((\mathbf{I} - \mathbf{T}_C^F \phi_C^{-1} \mathbf{T}_F^C \phi) -$
455 $\mathbf{I}) \phi^{-1} \chi + \mathbf{T}_C^F \phi_C^{-1} \mathbf{T}_F^C \chi = 0$.

¹⁴In some situations, *e.g.* when the transpose of linear interpolation is used for restriction (full-weighting), we do not get the identity in Assumption 4.2 but an invertible matrix. The same simplifications can be done, except one must take into account the inverse of $(\mathbf{T}_F^C \mathbf{T}_C^F)$.

¹⁵Note that the consistency condition is satisfied even without assumption 4.3.

456 **4.3. Two-level Time Multi-Grid.** Gander and Neumüller introduced TMG
 457 for discontinuous Galerkin approximations in time [25], which leads to a similar system
 458 as (2.12). We describe the two-level approach for general time discretizations, follow-
 459 ing their multi-level description [25, Sec. 3]. Consider a coarse problem defined as in
 460 Section 4.2 and a damped block Jacobi smoother as in Section 2.2.1 with relaxation
 461 parameter ω . Then, a two-level TMG iteration requires the following steps:

- 462 1. ν_1 pre-relaxation steps (2.15) with block Jacobi smoother,
- 463 2. one CGC (4.3) inverting the coarse grid operators,
- 464 3. ν_2 post-relaxation steps (2.15) with the block Jacobi smoother,

465 each corresponding to a block iteration. If we combine all these block iterations we
 466 do not obtain a primary block iteration but a more complex expression, of which the
 467 analysis is beyond the scope of this paper. However, a primary block iteration in the
 468 sense of Definition 2.5 is obtained when

- 469 • Assumption 4.3 holds, so that $\Delta_\chi = 0$,
- 470 • only one pre-relaxation step is used, $\nu_1 = 1$,
- 471 • and no post-relaxation step is considered, $\nu_2 = 0$.

472 Then, the two-level iteration reduces to the two block updates from (2.16) and (4.12),

$$473 \quad (4.13) \quad \mathbf{u}_{n+1}^{k+1/2} = (1 - \omega)\mathbf{u}_{n+1}^k + \omega\phi^{-1}\chi\mathbf{u}_n^k,$$

$$474 \quad (4.14) \quad \mathbf{u}_{n+1}^{k+1} = (\mathbf{I} - \mathbf{T}_C^F\phi_C^{-1}\mathbf{T}_F^C\phi)\mathbf{u}_{n+1}^{k+1/2} + \mathbf{T}_C^F\phi_C^{-1}\chi_C\mathbf{T}_F^C\mathbf{u}_n^{k+1},$$

476 using $k+1/2$ as intermediate index. Combining (4.13) and (4.14) leads to the primary
 477 block iteration

$$478 \quad (4.15) \quad \mathbf{u}_{n+1}^{k+1} = (\mathbf{I} - \mathbf{T}_C^F\phi_C^{-1}\mathbf{T}_F^C\phi) [(1 - \omega)\mathbf{u}_{n+1}^k + \omega\phi^{-1}\chi\mathbf{u}_n^k] + \mathbf{T}_C^F\phi_C^{-1}\chi_C\mathbf{T}_F^C\mathbf{u}_n^{k+1}.$$

479 If $\omega \neq 1$, all block operators in this primary block iteration are non-zero, and apply-
 480 ing Theorem 2.8 leads to the error bound (2.35). Since the latter is similar to the
 481 one obtained for PFASST in Section 5.5.2, we leave its comparison with numerical
 482 experiments to Section 5. For $\omega = 1$ we get the simplified iteration

$$483 \quad (4.16) \quad \mathbf{u}_{n+1}^{k+1} = (\phi^{-1}\chi - \mathbf{T}_C^F\phi_C^{-1}\mathbf{T}_F^C\chi)\mathbf{u}_n^k + \mathbf{T}_C^F\phi_C^{-1}\chi_C\mathbf{T}_F^C\mathbf{u}_n^{k+1},$$

484 and the following result:

485 **PROPOSITION 4.4.** *Consider a CGC as in Section 4.2, such that the prolongation*
 486 *and restriction operators (in time) satisfy Assumption 4.2. If Assumption 4.3 also*
 487 *holds and only one block Jacobi pre-relaxation step (2.15) with $\omega = 1$ is used before*
 488 *the CGC, then two-level TMG is equivalent to PARAREAL, where the coarse solver \mathcal{G}*
 489 *uses the same time integrator as the fine solver \mathcal{F} but with larger time steps, i.e.*

$$490 \quad (4.17) \quad \mathcal{G} := \mathbf{T}_C^F\phi_C^{-1}\mathbf{T}_F^C\chi.$$

491 This is a particular case of a result obtained before by Gander [26, Theorem 3.1] but is
 492 presented here in the context of our GFM framework and the definition of PARAREAL
 493 given in Section 3.1. In particular, it shows that the simplified two-grid iteration on
 494 (2.12) is equivalent to the preconditioned fixed-point iteration (3.6) of PARA-
 495 REAL if some conditions are met and $\tilde{\phi}^{-1} := \mathbf{T}_C^F\phi_C^{-1}\mathbf{T}_F^C$ is used as the approximate
 496 integration operator¹⁶. However, the TMG iteration here updates also the fine time

¹⁶Note that, even if $\mathbf{T}_C^F\phi_C^{-1}\mathbf{T}_F^C$ is not invertible, this abuse of notation is possible as (3.6) requires an approximation of ϕ^{-1} rather than an approximation of ϕ itself.

497 point values, using \mathbf{T}_C^F to interpolate the coarse values computed with ϕ_C , hence
 498 applying the PARAREAL update *to all volume values*. This is the only “difference”
 499 with the original definition of PARAREAL in [36], where the update is only applied to
 500 the interface value between blocks.

501 One key idea of STMG that we have not described yet is the block diagonal
 502 Jacobi smoother used for relaxation. Even if its diagonal blocks use a time integration
 503 operator identical to those of the fine problem (hence requiring the inversion of ϕ),
 504 their spatial part in STMG is approximated using one V-cycle multi-grid iteration in
 505 space based on a pointwise smoother [25, Sec. 4.3]. We do not cover this aspect in
 506 our description of TMG here, since we focus on time only, but describe in the next
 507 section a similar approach that is used for PFASST.

508 **5. Writing PFASST as a block iteration.** PFASST is also based on a TMG
 509 approach using an approximate relaxation step, but the approximation of the block
 510 Jacobi smoother is *done in time and not in space, in contrast to STMG*. In addition,
 511 the CGC in PFASST is also approximated, *i.e.* there is no direct solve on the coarse
 512 level to compute the CGC as in STMG. One PFASST iteration is therefore a combi-
 513 nation of an *Approximate Block Jacobi* (ABJ) smoother, see Section 5.2, followed by
 514 one (or more) ABGS iteration(s) of Section 2.2.2 on the coarse level to approximate
 515 the CGC [11, Sec. 3.2]. While we describe only the two-level variant, the algorithm
 516 can use more levels [11, 48]. The main component of PFASST is the approximation
 517 of the time integrator blocks using Spectral Deferred Corrections (SDC) [9], from
 518 which its other key components (ABJ and ABGS) are built. Hence we first describe
 519 how SDC is used to define an ABGS iteration in Section 5.1, then ABJ in Section 5.2,
 520 and finally PFASST in Section 5.3.

521 **5.1. Approximate Block Gauss-Seidel with SDC.** SDC can be seen as a
 522 preconditioner when integrating the ODE problem (2.1) with collocation methods,
 523 see Section 2.1.2. Consider the block operators

$$524 \quad (5.1) \quad \phi := (\mathbf{I} - \mathbf{Q}), \quad \chi := \mathbf{H} \quad \Longrightarrow \quad (\mathbf{I} - \mathbf{Q})\mathbf{u}_{n+1} = \mathbf{H}\mathbf{u}_n.$$

525 SDC approximates the quadrature matrix \mathbf{Q} by

$$526 \quad (5.2) \quad \mathbf{Q}_\Delta = \lambda\Delta t(\tilde{q}_{m,j}), \quad \tilde{q}_{m,j} = \int_0^{\tau_m} \tilde{l}_j(s)ds,$$

527 where \tilde{l}_j is an approximation of the Lagrange polynomial l_j . Usually, \mathbf{Q}_Δ is lower
 528 triangular [45, Sec 3] and easy to invert¹⁷. This approximation is used to build the
 529 preconditioned iteration

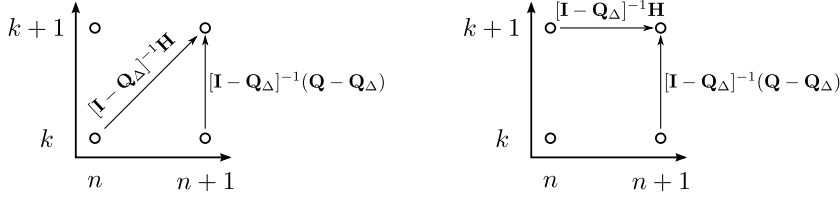
$$530 \quad (5.3) \quad \mathbf{u}_{n+1}^{k+1} = \mathbf{u}_{n+1}^k + [\mathbf{I} - \mathbf{Q}_\Delta]^{-1} (\mathbf{H}\mathbf{u}_n - (\mathbf{I} - \mathbf{Q})\mathbf{u}_{n+1}^k)$$

531 to solve (5.1), with \mathbf{u}_{n+1} as unknown. We obtain the generic preconditioned iteration
 532 for one block,

$$533 \quad (5.4) \quad \mathbf{u}_{n+1}^{k+1} = [\mathbf{I} - \tilde{\phi}^{-1}\phi] \mathbf{u}_{n+1}^k + \tilde{\phi}^{-1}\chi\mathbf{u}_n \quad \text{with} \quad \tilde{\phi} := \mathbf{I} - \mathbf{Q}_\Delta.$$

534 This shows that SDC inverts the ϕ operator approximately using $\tilde{\phi}$ block by block
 535 to solve the global problem (2.12), *i.e.* it fixes an n in (5.4), iterates over k until

¹⁷The notation \mathbf{Q}_Δ was chosen instead of $\tilde{\mathbf{Q}}$ for consistency with the literature, *cf.* [45, 3, 4].


 FIG. 6. kn -graphs for Block Jacobi SDC (left) and Block Gauss-Seidel SDC (right).

536 convergence, and then increments n by one. Hence SDC gives a natural way to define
 537 an approximate block integrator $\tilde{\phi}$ to be used to build ABJ and ABGS iterations.
 538 Defining the ABGS iteration (2.19) of Section 2.2.2 using the SDC block operators
 539 gives the block updating formula

$$540 \quad (5.5) \quad \mathbf{u}_{n+1}^{k+1} = \mathbf{u}_{n+1}^k + [\mathbf{I} - \mathbf{Q}_\Delta]^{-1} (\mathbf{H}\mathbf{u}_n^{k+1} - (\mathbf{I} - \mathbf{Q})\mathbf{u}_{n+1}^k),$$

541 which we call *Block Gauss-Seidel SDC* (BGS-SDC), very similar to (5.3) except that
 542 we use the new iterate \mathbf{u}_n^{k+1} and not the converged solution \mathbf{u}_n . This is a primary
 543 block iteration in the sense of Definition 2.5 with

$$544 \quad (5.6) \quad \begin{aligned} \mathbf{B}_1^0 &:= \mathbf{I} - [\mathbf{I} - \mathbf{Q}_\Delta]^{-1}(\mathbf{I} - \mathbf{Q}) = [\mathbf{I} - \mathbf{Q}_\Delta]^{-1}(\mathbf{Q} - \mathbf{Q}_\Delta), \\ \mathbf{B}_0^0 &:= 0, \quad \mathbf{B}_0^1 := [\mathbf{I} - \mathbf{Q}_\Delta]^{-1}\mathbf{H}, \end{aligned}$$

545 and its kn -graph is shown in Figure 6 (right).

546 **5.2. Approximate Block Jacobi with SDC.** Here we solve the global prob-
 547 lem (2.12) using a preconditioner that can be easily parallelized (Block Jacobi) and
 548 combine it with the approximation of the collocation operator ϕ by $\tilde{\phi}$ defined in (5.1)
 549 and (5.4). This leads to the *global* preconditioned iteration

$$550 \quad (5.7) \quad \mathbf{u}^{k+1} = \mathbf{u}^k + \mathbf{P}_{Jac}^{-1}(\mathbf{f} - \mathbf{A}\mathbf{u}^k), \quad \mathbf{P}_{Jac} = \begin{bmatrix} \tilde{\phi} & & \\ & \tilde{\phi} & \\ & & \ddots \end{bmatrix}.$$

551 This is equivalent to the block Jacobi relaxation in Section 2.2.1 with $\omega = 1$, except
 552 that the block operator ϕ is approximated by $\tilde{\phi}$. Using the SDC block operators (5.1)
 553 gives the block updating formula

$$554 \quad (5.8) \quad \mathbf{u}_{n+1}^{k+1} = \mathbf{u}_{n+1}^k + [\mathbf{I} - \mathbf{Q}_\Delta]^{-1} (\mathbf{H}\mathbf{u}_n^k - (\mathbf{I} - \mathbf{Q})\mathbf{u}_{n+1}^k),$$

555 which we call *Block Jacobi SDC* (BJ-SDC). This is a primary block iteration with

$$556 \quad (5.9) \quad \begin{aligned} \mathbf{B}_1^0 &:= \mathbf{I} - [\mathbf{I} - \mathbf{Q}_\Delta]^{-1}(\mathbf{I} - \mathbf{Q}) = [\mathbf{I} - \mathbf{Q}_\Delta]^{-1}(\mathbf{Q} - \mathbf{Q}_\Delta), \\ \mathbf{B}_0^0 &:= [\mathbf{I} - \mathbf{Q}_\Delta]^{-1}\mathbf{H}, \quad \mathbf{B}_0^1 := 0. \end{aligned}$$

557 Its kn -graph is shown in Figure 6 (left). This block iteration can be written in the
 558 more generic form

$$559 \quad (5.10) \quad \mathbf{u}_{n+1}^{k+1} = [\mathbf{I} - \tilde{\phi}^{-1}\phi] \mathbf{u}_{n+1}^k + \tilde{\phi}^{-1}\chi \mathbf{u}_n^k.$$

560 This is similar to (5.4) except that we use the current iterate \mathbf{u}_n^k from the previous
 561 block and not the converged solution \mathbf{u}_n . Note that ϕ and $\tilde{\phi}$ do not need to correspond
 562 to the SDC operators (5.1) and (5.4). This block iteration does not explicitly depend
 563 on the use of SDC, hence the name *Approximate Block Jacobi* (ABJ).

564 **5.3. PFASST.** We now give a simplified description of PFASST [11] applied to
 565 the Dahlquist problem (2.1). In particular, this corresponds to doing only one SDC
 566 sweep on the coarse level. To write PFASST as a block iteration, we first build
 567 the coarse level as in Section 4.2. From that we can form the $\tilde{\mathbf{Q}}$ quadrature matrix
 568 associated with the coarse nodes and the coarse matrix $\tilde{\mathbf{H}}$, as we would have done if
 569 we were using the collocation method of Section 2.1.2 on the coarse nodes. This leads
 570 to the definition of the ϕ_C and χ_C operators for the coarse level, combined with the
 571 transfer operators \mathbf{T}_F^C and \mathbf{T}_C^F , from which we can build the global matrices \mathbf{A}_C , $\bar{\mathbf{T}}_C^F$
 572 and $\bar{\mathbf{T}}_F^C$, see Section 4.2. Then we build the two-level PFASST iteration by defining
 573 a specific smoother and a modified CGC.

574 The smoother corresponds to a Block Jacobi SDC iteration (5.8) from Section 5.2
 575 to produce an intermediate solution

$$576 \quad (5.11) \quad \mathbf{u}_{n+1}^{k+1/2} = [\mathbf{I} - \mathbf{Q}_\Delta]^{-1}(\mathbf{Q} - \mathbf{Q}_\Delta)\mathbf{u}_{n+1}^k + [\mathbf{I} - \mathbf{Q}_\Delta]^{-1}\mathbf{H}\mathbf{u}_n^k,$$

577 denoted with iteration index $k + 1/2$. Using a CGC as in Section 4.2 would provide
 578 the global update formula

$$579 \quad (5.12) \quad \mathbf{A}_C \mathbf{d} = \bar{\mathbf{T}}_F^C(\mathbf{f} - \mathbf{A}\mathbf{u}^{k+1/2}),$$

$$580 \quad (5.13) \quad \mathbf{u}^{k+1} = \mathbf{u}^{k+1/2} + \bar{\mathbf{T}}_C^F \mathbf{d}.$$

582 Instead of a direct solve with \mathbf{A}_C to compute the defect \mathbf{d} , in PFASST one uses
 583 L Block Gauss-Seidel SDC iterations (or sweeps) to approximate it. Then (5.12)
 584 becomes

$$585 \quad (5.14) \quad \tilde{\mathbf{P}}_{GS} \mathbf{d}^\ell = (\tilde{\mathbf{P}}_{GS} - \mathbf{A}_C) \mathbf{d}^{\ell-1} + \bar{\mathbf{T}}_F^C(\mathbf{f} - \mathbf{A}\mathbf{u}^{k+1/2}), \quad \mathbf{d}^0 = 0, \quad \ell \in \{1, \dots, L\},$$

586 and reduces for one sweep only ($L = 1$) to

$$587 \quad (5.15) \quad \tilde{\mathbf{P}}_{GS} \mathbf{d} = \bar{\mathbf{T}}_F^C(\mathbf{f} - \mathbf{A}\mathbf{u}^{k+1/2}), \quad \tilde{\mathbf{P}}_{GS} = \begin{bmatrix} \tilde{\phi}_C & & \\ -\chi_C & \tilde{\phi}_C & \\ & \ddots & \ddots \end{bmatrix}.$$

588 Here $\tilde{\mathbf{P}}_{GS}$ correspond to the \mathbf{P}_{GS} preconditioning matrix, but written on the coarse
 589 level using an SDC-based approximation $\tilde{\phi}_C$ of the ϕ_C coarse time integrator. Com-
 590 bined with the prolongation on the fine level (5.13), we get the modified CGC update

$$591 \quad (5.16) \quad \mathbf{u}^{k+1} = \mathbf{u}^{k+1/2} + \bar{\mathbf{T}}_C^F \tilde{\mathbf{P}}_{GS}^{-1} \bar{\mathbf{T}}_F^C(\mathbf{f} - \mathbf{A}\mathbf{u}^{k+1/2}), \quad \tilde{\mathbf{P}}_{GS} = \begin{bmatrix} \tilde{\phi}_C & & \\ -\chi_C & \tilde{\phi}_C & \\ & \ddots & \ddots \end{bmatrix},$$

592 and together with (5.11) a two level method for the global system (2.12) [4, Sec. 2.2].
 593 Note that this is the same iteration we obtained for the CGC in Section 4.2, except
 594 that the coarse operator ϕ_C has been replaced by $\tilde{\phi}_C$. Assumption 4.3 holds, since
 595 using Lobatto or Radau-II nodes means \mathbf{H} has the form (2.11), which implies

$$596 \quad (5.17) \quad \Delta_\chi = \mathbf{T}_F^C \mathbf{H} - \tilde{\mathbf{H}} \mathbf{T}_F^C = 0.$$

597 Using similar computations as in Section 4.2 and the block operators defined for
 598 collocation and SDC (*cf.* Section 2.1.2 and Section 5.1) we obtain the block iteration

$$599 \quad (5.18) \quad \mathbf{u}_{n+1}^{k+1} = [\mathbf{I} - \mathbf{T}_C^F(\mathbf{I} - \tilde{\mathbf{Q}}_\Delta)^{-1} \mathbf{T}_F^C(\mathbf{I} - \mathbf{Q})] \mathbf{u}_{n+1}^{k+1/2} + \mathbf{T}_C^F(\mathbf{I} - \tilde{\mathbf{Q}}_\Delta)^{-1} \mathbf{T}_F^C \mathbf{H} \mathbf{u}_n^{k+1}$$

	Smoother		
CGC		Block Jacobi ($\omega = 1$)	Approximate Block Jacobi
Direct Solver		TMG ($\omega = 1$)	TMG _f
ABGS (one step)		TMG _c	Two-level PFASST

TABLE 1

Classification of two-level TMG methods, depending on their smoother for fine-level relaxation and computation of the Coarse Grid Correction (CGC).

600 by substitution into (4.12). Finally, the combination of the two gives

$$\begin{aligned}
 \mathbf{u}_{n+1}^{k+1} &= [\mathbf{I} - \mathbf{T}_C^F(\mathbf{I} - \tilde{\mathbf{Q}}_\Delta)^{-1}\mathbf{T}_F^C(\mathbf{I} - \mathbf{Q})][\mathbf{I} - \mathbf{Q}_\Delta]^{-1}(\mathbf{Q} - \mathbf{Q}_\Delta)\mathbf{u}_{n+1}^k \\
 &+ (\mathbf{I} - \mathbf{T}_C^F[\mathbf{I} - \tilde{\mathbf{Q}}_\Delta]^{-1}\mathbf{T}_F^C(\mathbf{I} - \mathbf{Q}))[\mathbf{I} - \mathbf{Q}_\Delta]^{-1}\mathbf{H}\mathbf{u}_n^k \\
 &+ \mathbf{T}_C^F(\mathbf{I} - \tilde{\mathbf{Q}}_\Delta)^{-1}\mathbf{T}_F^C\mathbf{H}\mathbf{u}_n^{k+1}.
 \end{aligned}
 \tag{5.19}$$

602 Using the generic formulation with the ϕ operators gives¹⁸

$$\begin{aligned}
 \mathbf{u}_{n+1}^{k+1} &= [\mathbf{I} - \mathbf{T}_C^F\tilde{\phi}_C^{-1}\mathbf{T}_F^C\phi](\mathbf{I} - \tilde{\phi}^{-1}\phi)\mathbf{u}_{n+1}^k \\
 &+ (\mathbf{I} - \mathbf{T}_C^F\tilde{\phi}_C^{-1}\mathbf{T}_F^C\phi)\tilde{\phi}^{-1}\chi\mathbf{u}_n^k + \mathbf{T}_C^F\tilde{\phi}_C^{-1}\mathbf{T}_F^C\chi\mathbf{u}_n^{k+1}.
 \end{aligned}
 \tag{5.20}$$

604 This is again a primary block iteration in the sense of Definition 2.5, but in contrast
 605 to most previously described block iterations, all block operators are non-zero.

606 **5.4. Similarities between PFASST, TMG and Parareal.** From the de-
 607 scription in the previous section, it is clear that PFASST is very similar to TMG.
 608 While TMG uses a (damped) block Jacobi smoother for pre-relaxation and a direct
 609 solve for the CGC, PFASST uses instead an approximate Block Jacobi smoother,
 610 and solves the CGC using one (or more) ABGS iterations on the coarse grid. This
 611 interpretation was obtained by Bolten et al. [3, Theorem 1], but is derived here using
 612 the GFM framework, and we summarize those differences in Table 1. Changing only
 613 the CGC or the smoother in TMG with $\omega = 1$ in contrast to both like in PFASST pro-
 614 duces two further PinT algorithms. We call those TMG_c (replacing the coarse solver
 615 by one step of ABGS) and TMG_f (replacing the fine Block Jacobi solver by ABJ).
 616 Note that TMG_c can be interpreted as PARAREAL using an approximate integration
 617 operator and larger time step for the coarse propagator if we set

$$\mathcal{G} := \mathbf{T}_C^F\tilde{\phi}_C^{-1}\mathbf{T}_F^C\chi.
 \tag{5.21}$$

619 Thus, the version of PARAREAL used in Section 3.2 is equivalent to TMG_c, and differs
 620 from PFASST only by the type of smoother used on the fine level.

621 **5.5. Analysis and numerical experiments.**

622 **5.5.1. Convergence of PFASST iteration components.** Since Block Jacobi
 623 SDC (5.8) can be written as a primary block iteration, we can apply Theorem 2.8
 624 with $\beta = 0$ to get the error bound

$$e_{n+1}^k \leq \begin{cases} \delta(\gamma + \alpha)^k & \text{if } k \leq n \\ \delta\gamma^k \sum_{i=0}^n \binom{n}{i} \left(\frac{\alpha}{\gamma}\right)^i & \text{otherwise,} \end{cases}
 \tag{5.22}$$

¹⁸We implicitly use $[\mathbf{I} - \mathbf{Q}_\Delta]^{-1}(\mathbf{Q} - \mathbf{Q}_\Delta) = \mathbf{I} - [\mathbf{I} - \mathbf{Q}_\Delta]^{-1}(\mathbf{I} - \mathbf{Q}) = \mathbf{I} - \tilde{\phi}^{-1}\phi$, see (5.6).

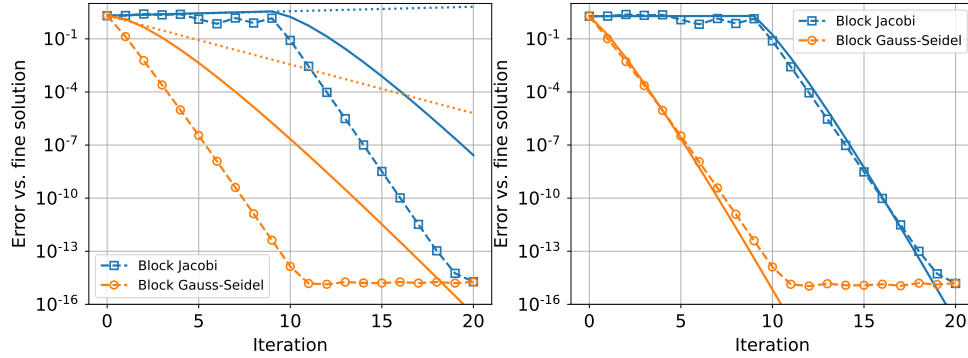


FIG. 7. Comparison of numerical errors with GFM-bounds for Block Jacobi SDC and Block Gauss-Seidel SDC. Left: error on the block variables (dashed), GFM-bounds (solid), linear bound from the iteration matrix (dotted). Right: error estimate using the interface approximation from Corollary 2.9. Note that the numerical errors on block variables (left) and at the interface (right) are close but not identical (see Remark 2.10).

626 with $\gamma := \|\mathbf{I} - \mathbf{Q}_\Delta\|^{-1}(\mathbf{Q} - \mathbf{Q}_\Delta)\|$, $\alpha := \|\mathbf{I} - \mathbf{Q}_\Delta\|^{-1}\mathbf{H}\|$. Note that γ is proportional
 627 to $\lambda\Delta t$ through the $\mathbf{Q} - \mathbf{Q}_\Delta$ term and for small Δt , α tends to $\|\mathbf{H}\|$ which is constant.
 628 We can identify two convergence regimes: for early iterations ($k \leq n$), the bound does
 629 not contract if $\gamma + \alpha \geq 1$ (which is generally the case). For later iterations ($k > n$), a
 630 small-enough time step leads to convergence of the algorithm through the γ^k factor.
 631 Similarly, for Block Gauss-Seidel SDC (5.5), Theorem 2.8 with $\alpha = 0$ gives

$$632 \quad (5.23) \quad e_{n+1}^k \leq \delta \frac{\gamma^k}{(k-1)!} \sum_{i=0}^n \prod_{l=1}^{k-1} (i+l)\beta^i,$$

633 where $\gamma := \|\mathbf{I} - \mathbf{Q}_\Delta\|^{-1}(\mathbf{Q} - \mathbf{Q}_\Delta)\|$, $\beta := \|\mathbf{I} - \mathbf{Q}_\Delta\|^{-1}\mathbf{H}\|$. This iteration contracts
 634 already in early iterations if γ is small enough. Since the value for γ is the same
 635 for both Block Gauss-Seidel SDC and Block Jacobi-SDC, both algorithms have an
 636 asymptotically similar convergence rate.

637 We illustrate this with the following example. Let $\lambda := i$, $u_0 := 1$, and let the
 638 time interval $[0, \pi]$ be divided into $N = 10$ sub-intervals. Inside each sub-interval,
 639 we use one step of the collocation method from Section 2.1.2 with $M := 10$ Lobatto-
 640 Legendre nodes [27]. This gives us block variables of size $M = 10$ and we choose \mathbf{Q}_Δ
 641 as the matrix defined by a single Backward Euler step between nodes to build the ϕ
 642 operator. The starting value \mathbf{u}^0 for the iteration is initialized with random numbers
 643 starting from the same seed. Figure 7 (left) shows the numerical error for the last
 644 block using the L^∞ norm, the bound obtained with the GFM method and the linear
 645 bound using the norm of the global iteration matrix. As for PARAREAL in Section 3.2,
 646 the GFM-bound is similar to the iteration matrix bound for the first few iterations,
 647 but much tighter for later iterations. In particular, the linear bound cannot show the
 648 change in convergence regime of the Block Jacobi SDC iteration (after $k = 10$) but
 649 the GFM-bound does. Also, we observe that while the GFM-bound overestimates the
 650 error, the interface approximation of Corollary 2.9 gives a very good estimate of the
 651 error at the interface, see Figure 7 (right).

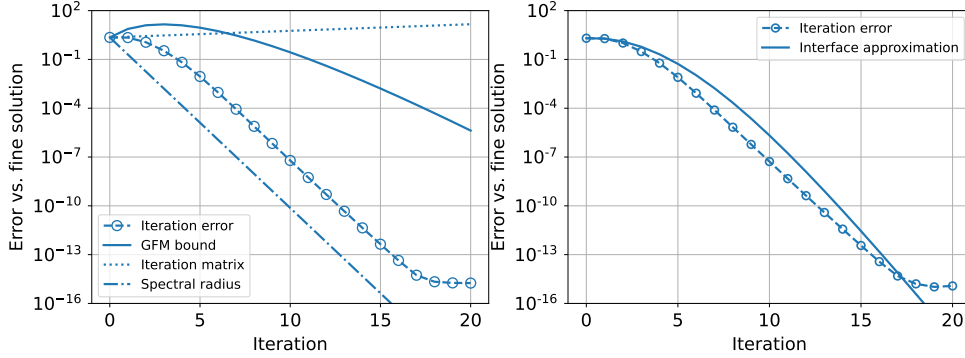


FIG. 8. Comparison of numerical errors with GFM-bounds for PFASST. Left: error bound using volume values. Right: estimate using the interface approximation. Note that the numerical errors on block variables (left) and at the interface (right) are very close but not identical (see Remark 2.10).

652 **5.5.2. Analysis and convergence of PFASST.** The GFM framework pro-
 653 vides directly an error bound for PFASST: applying Theorem 2.8 to (5.19) gives

$$654 \quad (5.24) \quad e_{n+1}^k \leq \delta \gamma^k \sum_{i=0}^{\min(n,k)} \sum_{l=0}^{n-i} \binom{k}{i} \binom{l+k-1}{l} \left(\frac{\alpha}{\gamma}\right)^i \beta^l,$$

655 with $\gamma := \|[\mathbf{I} - \mathbf{T}_C^F(\mathbf{I} - \tilde{\mathbf{Q}}_\Delta)^{-1} \mathbf{T}_F^C(\mathbf{I} - \mathbf{Q})][\mathbf{I} - \mathbf{Q}_\Delta]^{-1}(\mathbf{Q} - \mathbf{Q}_\Delta)\|$, $\beta := \|\mathbf{T}_C^F(\mathbf{I} -$
 656 $\tilde{\mathbf{Q}}_\Delta)^{-1} \tilde{\mathbf{H}} \mathbf{T}_F^C\|$, and $\alpha := \|(\mathbf{I} - \mathbf{T}_C^F[\mathbf{I} - \tilde{\mathbf{Q}}_\Delta]^{-1} \mathbf{T}_F^C(\mathbf{I} - \mathbf{Q}))[\mathbf{I} - \mathbf{Q}_\Delta]^{-1} \mathbf{H}\|$.

657 We compare this bound with numerical experiments. Let $\lambda := i$, $u_0 := 1$. The
 658 time interval $[0, 2\pi]$ for the Dahlquist problem (2.1) is divided into $N = 10$ sub-
 659 intervals. Inside each sub-interval we use $M := 6$ Lobatto-Legendre nodes on the fine
 660 level and $M_C := 2$ Lobatto nodes on the coarse level. The \mathbf{Q}_Δ and $\tilde{\mathbf{Q}}_\Delta$ operators use
 661 Backward Euler. In Figure 8 (left) we compare the measured numerical error with the
 662 GFM-bound and the linear bound from the iteration matrix. As in Section 5.5.1, both
 663 bounds overestimate the numerical error, even if the GFM-bound shows convergence
 664 for the later iterations, which the linear bound from the iteration matrix cannot. We
 665 also added an error estimate built using the spectral radius of the iteration matrix,
 666 for which an upper bound was derived in [4]. For this example, the spectral radius
 667 reflects the asymptotic convergence rate for the last iterations better than GFM.
 668 This highlights a weakness of the current GFM-bound: applying norm and triangle
 669 inequalities to the vector error recurrence (2.25) can induce a large approximation
 670 error in the scalar error recurrence (2.26) that is then solved with generating functions.
 671 Improving this is planned for future work.

672 However, one advantage of the GFM-bound over the spectral radius is its generic
 673 aspect allowing it to be applied to many iterative algorithms, even those having an
 674 iteration matrix with spectral radius equal to zero like PARAREAL [44]. Further-
 675 more, the interface approximation from Corollary 2.9 allows us to get a significantly
 676 better estimation of the numerical error, as shown in Figure 8 (right). For the GFM-
 677 bound we have $(\alpha, \beta, \gamma) = (0.16, 1, 0.19)$, while for the interface approximation we get
 678 $(\bar{\alpha}, \bar{\beta}, \bar{\gamma}) = (0.16, 0.84, 0.02)$. In the second case, since $\bar{\gamma}$ is one order smaller than the
 679 other coefficients, we get an error estimate that is closer to the one for PARAREAL in
 680 Section 3.2 where $\gamma = 0$. This similarity between PFASST and PARAREAL (cf. Sec-
 681 tion 5.4) will be highlighted in the next section.

Algorithm	$\mathbf{B}_1^0(\mathbf{u}_{n+1}^k)$	$\mathbf{B}_0^0(\mathbf{u}_n^k)$	$\mathbf{B}_0^1(\mathbf{u}_{n+1}^k)$
damped Block Jacobi	$\mathbf{I} - \omega \mathbf{I}$	$\omega \phi^{-1} \chi$	-
ABJ	$\mathbf{I} - \tilde{\phi}^{-1} \phi$	$\tilde{\phi}^{-1} \chi$	-
ABGS	$\mathbf{I} - \tilde{\phi}^{-1} \phi$	-	$\tilde{\phi}^{-1} \chi$
PARAREAL	-	$(\phi^{-1} - \tilde{\phi}^{-1}) \chi$	$\tilde{\phi}^{-1} \chi$
TMG	$(1 - \omega)(\mathbf{I} - \mathbf{T}_C^F \phi_C^{-1} \mathbf{T}_F^C \phi)$	$\omega(\phi^{-1} - \mathbf{T}_C^F \phi_C^{-1} \mathbf{T}_F^C) \chi$	$\mathbf{T}_C^F \phi_C^{-1} \mathbf{T}_F^C \chi$
TMG _c	-	$(\phi^{-1} - \mathbf{T}_C^F \tilde{\phi}_C^{-1} \mathbf{T}_F^C) \chi$	$\mathbf{T}_C^F \tilde{\phi}_C^{-1} \mathbf{T}_F^C \chi$
TMG _f	$(\mathbf{I} - \mathbf{T}_C^F \phi_C^{-1} \mathbf{T}_F^C \phi)(\mathbf{I} - \tilde{\phi}^{-1} \phi)$	$(\tilde{\phi}^{-1} - \mathbf{T}_C^F \phi_C^{-1} \mathbf{T}_F^C \phi \tilde{\phi}^{-1}) \chi$	$\mathbf{T}_C^F \phi_C^{-1} \mathbf{T}_F^C \chi$
PFASST	$(\mathbf{I} - \mathbf{T}_C^F \tilde{\phi}_C^{-1} \mathbf{T}_F^C \phi)(\mathbf{I} - \tilde{\phi}^{-1} \phi)$	$(\tilde{\phi}^{-1} - \mathbf{T}_C^F \tilde{\phi}_C^{-1} \mathbf{T}_F^C \phi \tilde{\phi}^{-1}) \chi$	$\mathbf{T}_C^F \tilde{\phi}_C^{-1} \mathbf{T}_F^C \chi$

TABLE 2

Summary of all the methods we analyzed, and their block iteration operators. Note that TMG with $\omega = 1$ and TMG_c corresponds to PARAREAL with a specific choice of the coarse propagator.

	$\phi^{-1} \chi$	$\tilde{\phi}^{-1} \chi$	$\mathbf{T}_C^F \phi_C^{-1} \mathbf{T}_F^C \chi$	$\mathbf{T}_C^F \tilde{\phi}_C^{-1} \mathbf{T}_F^C \chi$
Figure 9 (left)	$1.20e^{-5}$	$3.57e^{-1}$	$1.19e^{-2}$	$4.87e^{-1}$
Figure 9 (right)	$3.14e^{-4}$	$6.24e^{-2}$	$5.14e^{-3}$	$2.67e^{-1}$

TABLE 3

Maximum error over time for each block propagator run sequentially. The first column shows the error of the fine propagator, while the next three columns show the error of the three possible approximate propagators. In the top row, ϕ corresponds to a collocation method with $M = 5$ nodes while ϕ_C is a collocation method with $M = 3$ nodes. $\tilde{\phi}$ is a backward Euler method with $M = 5$ steps per block while $\tilde{\phi}_C$ is backward Euler with $M = 3$ steps per block. In the bottom row, ϕ corresponds to $M = 5$ uniform steps per block of a 4th order Runge-Kutta method, ϕ_C is the same method with $M = 3$ steps per block. $\tilde{\phi}$ is a 2nd order Runge-Kutta method (Heun) with $M = 5$ uniform steps per block while $\tilde{\phi}_C$ is the same method with $M = 3$ uniform time steps per block.

6. Comparison of iterative PinT algorithms.

Using the notation of the GFM framework, we provide the primary block iterations of all iterative PinT algorithm investigated throughout this paper in Table 2. In particular, the first rows summarize the basic block iterations used as components to build the iterative PinT methods. While damped Block Jacobi (Section 2.2.1) and ABJ (Section 5.2) are more suitable for smoothing¹⁹, ABGS (Section 2.2.2) is mostly used as solver (*e.g.* to compute the CGC). This allows us to compare the convergence of each block iteration, and we illustrate this with the following examples.

We consider the Dahlquist problem with $\lambda := 2i - 0.2$, $u_0 = 1$. First, we decompose the simulation interval $[0, 2\pi]$ into $N = 10$ sub-intervals. Next, we choose a block discretization with $M = 5$ Lobatto-Legendre nodes, a collocation method on each block for fine integrator ϕ , see Section 2.1.2. We build a coarse block discretization using $M_C = 3$, and define on each level an approximate integrator using Backward Euler. This allows us to define the $\tilde{\phi}$, ϕ_C and $\tilde{\phi}_C$ integrators, see the legend of Table 3 for more details, where we show the maximum absolute error in time for each of the four propagators run sequentially. The high order collocation method with $M = 5$ nodes $\phi^{-1} \chi$ is the most accurate. The coarse collocation method with

¹⁹Note that algorithms used as smoother have $\mathbf{B}_0^1 = 0$, which is a necessary condition for parallel computation across all blocks.

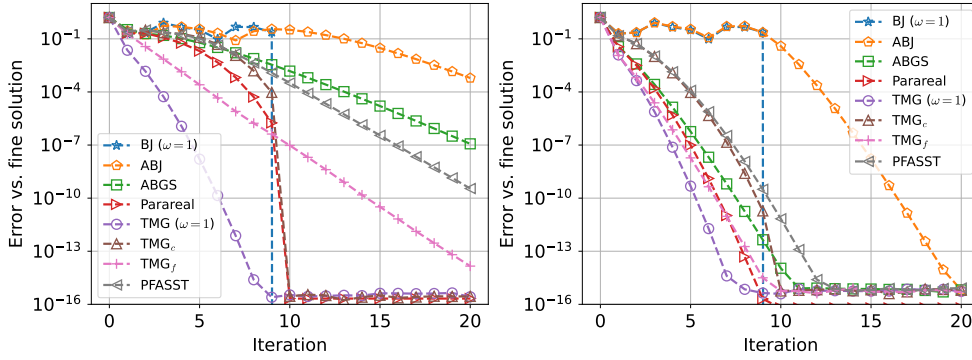


FIG. 9. Comparison of iterative methods convergence using the GFM framework. Left: collocation as fine integrator. Right: 4th order Runge-Kutta method as fine integrator. PARAREAL ($\omega=1$) and PARAREAL (TMG_c) denote a specific coarse propagator for PARAREAL.

699 $M = 3$ nodes interpolated to the fine mesh is still more accurate than the backward
 700 Euler method with $M = 5$ nodes $\tilde{\phi}^{-1}\chi$ or the backward Euler method with $M = 3$
 701 interpolated to the fine mesh. Then we run all algorithms in Table 2, initializing the
 702 block variable iterate with the same random initial guess. The error for the last block
 703 variable with respect to the fine sequential solution is shown in Figure 9 (left). In
 704 addition, we show the same results in Figure 9 (right), but using the classical 4th order
 705 Runge-Kutta method as fine propagator, 2nd order Runge-Kutta (Heun method) for
 706 the approximate integration operator and equidistant points using a volume formula-
 707 tion as described in Section 2.1.1. Note that PARAREAL, TMG _{$\omega=1$} and TMG_c are
 708 each PARAREAL algorithms using respectively $\tilde{\phi}^{-1}\chi$, $\mathbf{T}_C^F \tilde{\phi}_C^{-1} \mathbf{T}_F^C \chi$ and $\mathbf{T}_C^F \tilde{\phi}_C^{-1} \mathbf{T}_F^C \chi$
 709 as coarse propagator \mathcal{G} (see Table 3 for their discretization error).

710 The TMG iteration converges fastest, since it uses the most accurate block inte-
 711 grators on both levels, cf. Table 3. Keeping the same CGC but approximating the
 712 smoother, TMG_f improves the first iterations, but convergence for later iterations
 713 is closer to PFASST. This suggests that convergence for later iterations is mostly
 714 governed by the accuracy of the smoother since both TMG_f and PFASST use ABJ.
 715 This is corroborated by the comparison of PFASST and TMG_c, which differ only
 716 in their choice of smoother. While the exact Block Jacobi relaxation makes TMG_c
 717 converge after $k = N$ iterations (a well known property of PARAREAL), using the ABJ
 718 smoother means that PFASST does not share this property.

719 On the other hand, the first iterations are also influenced by the CGC accuracy.
 720 The iteration error is very similar for PFASST and TMG_c which have the same
 721 CGC. This is more pronounced when using the 4th order Runge-Kutta method for ϕ ,
 722 as we see in Figure 9 (right). Early iteration errors are similar for two-level methods
 723 that use the same CGC (TMG/ TMG_f, and PFASST/ TMG_c). Similarities of the
 724 first iteration errors can also be observed for PARAREAL and ABGS. Both algorithms
 725 use the same \mathbf{B}_0^1 operator, see Table 2. This suggests that early iteration errors
 726 are mostly governed by the accuracy of \mathbf{B}_0^1 , which is corroborated by the two-level
 727 methods (TMG and TMG_f use the same \mathbf{B}_0^1 operator, as PFASST and TMG_c).

728 *Remark 6.1.* An important aspect of this analysis is that it compares *only the*
 729 *convergence* of each algorithm, and not their overall computational cost. For in-
 730 stance, PFASST and TMG_c appear to be equivalent for the first iterations, but the
 731 block iteration of PFASST is cheaper than TMG_c, because an approximate block

integrator is used for relaxation. To account for this and build a model for computational efficiency, the GFM framework would need to be combined with a model for computational cost of the different parts in the block iterations. Such a study is beyond the scope of this paper but is the subject of ongoing work.

7. Conclusion. We have shown that the Generating Function Method (GFM) can be used to compare convergence of different iterative PinT algorithms. To do so, we formulated popular methods like PARAREAL, PFASST, MGRIT or TMG in a common framework based on the definition of a primary block iteration. The GFM analysis showed that all these methods eventually converge super-linearly²⁰ due to the evolution nature of the problems. We confirmed this by numerical experiments and our PYTHON code is publically available²¹.

Our analysis opens up further research directions. For example, studying multi-step block iterations like MGRIT with FCF-relaxation and more complex two-level methods without Assumption 4.3 would be a useful extension of the GFM framework. Similarly, an extension to multi-level versions of STMG, PFASST and MGRIT would be very valuable. Finally, in practice PinT methods are used to solve space-time problems. The GFM framework should be able to provide convergence bounds in this case as well, potentially even for non-linear problems, considering GFM was used successfully to study PARAREAL applied to non-linear systems of ODEs [21].

Acknowledgments. We greatly appreciate the very detailed feedback from the anonymous reviewers. It helped a lot to improve the organization of the paper and to make it more accessible.

Appendix A. Error bounds for *Primary Block Iterations*.

A.1. Incomplete Primary Block Iterations. First, we consider

$$(A.1) \quad (\text{PBI-1}) : \quad \mathbf{u}_{n+1}^{k+1} = \mathbf{B}_0^1(\mathbf{u}_n^{k+1}) + \mathbf{B}_0^0(\mathbf{u}_n^k),$$

$$(A.2) \quad (\text{PBI-2}) : \quad \mathbf{u}_{n+1}^{k+1} = \mathbf{B}_1^0(\mathbf{u}_{n+1}^k) + \mathbf{B}_0^0(\mathbf{u}_n^k),$$

$$(A.3) \quad (\text{PBI-3}) : \quad \mathbf{u}_{n+1}^{k+1} = \mathbf{B}_1^0(\mathbf{u}_{n+1}^k) + \mathbf{B}_0^1(\mathbf{u}_n^{k+1}),$$

where one block operator is zero. (PBI-1) corresponds to PARAREAL, (PBI-2) to Block Jacobi SDC and (PBI-3) to Block Gauss-Seidel SDC. We recall the notations :

$$(A.4) \quad \alpha := \|\mathbf{B}_0^0\|, \quad \beta := \|\mathbf{B}_0^1\|, \quad \gamma := \|\mathbf{B}_1^0\|.$$

Application of Lemma 2.7 gives the recurrence relations

$$(A.5) \quad (\text{PBI-1}) : \quad \rho_{k+1}(\zeta) \leq \frac{\alpha\zeta}{1-\beta\zeta}\rho_k(\zeta) \implies \rho_k(\zeta) \leq \alpha^k \left(\frac{\zeta}{1-\beta\zeta} \right)^k \rho_0(\zeta)$$

$$(A.6) \quad (\text{PBI-2}) : \quad \rho_{k+1}(\zeta) \leq (\gamma + \alpha\zeta)\rho_k(\zeta) \implies \rho_k(\zeta) \leq \gamma^k \left(1 + \frac{\alpha}{\gamma}\zeta \right)^k \rho_0(\zeta)$$

$$(A.7) \quad (\text{PBI-3}) : \quad \rho_{k+1}(\zeta) \leq \frac{\gamma}{1-\beta\zeta}\rho_k(\zeta) \implies \rho_k(\zeta) \leq \gamma^k \frac{1}{(1-\beta\zeta)^k} \rho_0(\zeta)$$

²⁰This is due to the factorial term stemming from the binomial sums in the estimates (2.32)-(2.35).

²¹<https://github.com/Parallel-in-Time/gfm>

768 for the corresponding generating functions. Using definition²² (2.30) for δ , we find
 769 that $\rho_0(\zeta) \leq \delta \sum_{n=0}^{\infty} \zeta^{n+1}$. By using the binomial series expansion

$$770 \quad (\text{A.8}) \quad \frac{1}{(1-\beta\zeta)^k} = \sum_{n=0}^{\infty} \binom{n+k-1}{n} (\beta\zeta)^n$$

771 for $k > 0$ and the Newton binomial sum, we obtain for the three block iterations

$$772 \quad (\text{A.9}) \quad (\text{PBI-1}) : \quad \rho_k(\zeta) \leq \delta \alpha^k \zeta \left[\sum_{n=0}^{\infty} \binom{n+k-1}{n} \beta^n \zeta^{n+k} \right] \left[\sum_{n=0}^{\infty} \zeta^n \right]$$

$$773 \quad (\text{A.10}) \quad (\text{PBI-2}) : \quad \rho_k(\zeta) \leq \delta \gamma^k \zeta \left[\sum_{n=0}^k \binom{k}{n} \left(\frac{\alpha}{\gamma} \right)^n \zeta^n \right] \left[\sum_{n=0}^{\infty} \zeta^n \right]$$

$$774 \quad (\text{A.11}) \quad (\text{PBI-3}) : \quad \rho_k(\zeta) \leq \delta \gamma^k \zeta \left[\sum_{n=0}^{\infty} \binom{n+k-1}{n} \beta^n \zeta^n \right] \left[\sum_{n=0}^{\infty} \zeta^n \right].$$

776 *Error bound for PBI-1.* We simplify the expression using

$$777 \quad (\text{A.12}) \quad \left[\sum_{n=0}^{\infty} \binom{n+k-1}{n} \beta^n \zeta^{n+k} \right] = \left[\sum_{n=k}^{\infty} \binom{n-1}{n-k} \beta^{n-k} \zeta^n \right],$$

778 and then the series product formula

$$779 \quad (\text{A.13}) \quad \left[\sum_{n=0}^{\infty} a_n \zeta^n \right] \left[\sum_{n=0}^{\infty} b_n \zeta^n \right] = \sum_{n=0}^{\infty} c_n \zeta^n, \quad c_n = \sum_{i=0}^n a_i b_{n-i},$$

780 with $b_n = 1$ and

$$781 \quad (\text{A.14}) \quad a_n = \begin{cases} 0 & \text{if } n < k, \\ \binom{n-1}{n-k} \beta^{n-k} & \text{otherwise.} \end{cases}$$

783 From this we get

$$784 \quad (\text{A.15}) \quad c_n = \sum_{i=k}^n \binom{i-1}{i-k} \beta^{i-k} = \sum_{i=0}^{n-k} \binom{i+k-1}{i} \beta^i = \sum_{i=0}^{n-k} \frac{\prod_{l=1}^{k-1} (i+l)}{(k-1)!} \beta^i,$$

785 using the convention that the product reduces to one when there are no terms in it.

786 Identifying coefficients in the power series and rearranging terms yields for $k > 0$

$$787 \quad (\text{A.16}) \quad \boxed{(\text{PBI-1}) : \quad e_{n+1}^k \leq \delta \frac{\alpha^k}{(k-1)!} \sum_{i=0}^{n-k} \prod_{l=1}^{k-1} (i+l) \beta^i.}$$

788 Following an idea by Gander and Hairer [21], we can also consider the error recurrence
 789 $e_{n+1}^{k+1} \leq \alpha e_n^k + \beta e_n^{k+1}$, $\beta = \max(1, \beta)$. Using the upper bound $\sum_{n=0}^{\infty} \zeta^n = \frac{1}{1-\zeta} \leq \frac{1}{1-\beta\zeta}$,

²²The definition of δ as maximum error for $n \in \{0, \dots, N\}$ can be extended to $n \in \mathbb{N}$, as the error values for $n > N$ do not matter and can be set to zero.

790 for the initial error, we avoid the series product and get $\rho_k(\zeta) \leq \delta \alpha^k \frac{\zeta^k}{(1-\beta)^{k+1}}$ as bound
 791 on the generating function. We then obtain the simpler error bound

$$792 \quad (\text{A.17}) \quad e_{n+1}^k \leq \delta \frac{\alpha^k}{k!} \bar{\beta}^{n-k} \prod_{l=1}^k (n+1-l)$$

793 as in the proof of [21, Th. 1].

794 *Error bound for PBI-2.* We use (A.13) again with $b_n = 1$ to get

$$795 \quad (\text{A.18}) \quad a_n = \begin{cases} \binom{k}{n} \left(\frac{\alpha}{\gamma}\right)^n & \text{if } n \leq k, \\ 0 & \text{otherwise.} \end{cases}$$

797 From this we get $c_n = \sum_{i=0}^{\min(n,k)} \binom{k}{i} \left(\frac{\alpha}{\gamma}\right)^i$, which yields for $k > 0$ the error bound

$$798 \quad (\text{A.19}) \quad (\text{PBI-2}) : \quad e_{n+1}^k \leq \begin{cases} \delta(\gamma + \alpha)^k & \text{if } k \leq n, \\ \delta \gamma^k \sum_{i=0}^n \binom{k}{i} \left(\frac{\alpha}{\gamma}\right)^i & \text{otherwise.} \end{cases}$$

799 *Error bound for PBI-3.* We use (A.13) with $b_n = 1$ for the series product to get

$$800 \quad (\text{A.20}) \quad a_n = \binom{n+k-1}{n} \beta^n = \frac{\prod_{l=1}^{k-1} (n+l)}{(k-1)!} \beta^n,$$

802 which yields the error bound

$$803 \quad (\text{A.21}) \quad (\text{PBI-3}) : \quad e_{n+1}^k \leq \delta \frac{\gamma^k}{(k-1)!} \sum_{i=0}^n \prod_{l=1}^{k-1} (i+l) \beta^i$$

804 for $k > 0$.

805 **A.2. Full Primary Block Iteration.** We now consider a primary block itera-
 806 tion (2.13) with all block operators non-zero,

$$807 \quad (\text{A.22}) \quad (\text{PBI-Full}) : \quad \mathbf{u}_{n+1}^{k+1} = \mathbf{B}_1^0(\mathbf{u}_{n+1}^k) + \mathbf{B}_0^1(\mathbf{u}_n^{k+1}) + \mathbf{B}_0^0(\mathbf{u}_n^k),$$

808 with α , β and γ defined in (A.4). Applying Lemma 2.7 leads to

$$809 \quad (\text{A.23}) \quad \rho_{k+1}(\zeta) \leq \frac{\gamma + \alpha\zeta}{1 - \beta\zeta} \rho_k(\zeta) \implies \rho_k(\zeta) \leq \left(\frac{\gamma + \alpha\zeta}{1 - \beta\zeta}\right)^k \rho_0(\zeta).$$

810 Combining the calculations performed for PBI-2 and PBI-3, we obtain

$$811 \quad (\text{A.24}) \quad \rho_k(\zeta) \leq \delta \zeta \gamma^k \left[\sum_{n=0}^k \binom{k}{n} \left(\frac{\alpha}{\gamma}\right)^n \zeta^n \right] \left[\sum_{n=0}^{\infty} \binom{n+k-1}{n} \beta^n \zeta^n \right] \left[\sum_{n=0}^{\infty} \zeta^n \right]$$

$$812 \quad (\text{A.25}) \quad = \delta \zeta \gamma^k \left[\sum_{n=0}^k \binom{k}{n} \left(\frac{\alpha}{\gamma}\right)^n \zeta^n \right] \left[\sum_{n=0}^{\infty} \sum_{i=0}^n \binom{i+k-1}{i} \beta^i \zeta^n \right].$$

813

814 Then using (A.13) with

$$815 \quad (A.26) \quad a_n = \begin{cases} \binom{k}{n} \left(\frac{\alpha}{\gamma}\right)^n & \text{if } n \leq k, \\ 0 & \text{otherwise,} \end{cases} \quad b_n = \sum_{i=0}^n \binom{i+k-1}{i} \beta^i,$$

816 we obtain

$$817 \quad (A.27) \quad \rho_k(\zeta) \leq \delta \zeta \gamma^k \sum_{n=0}^{\infty} c_n \zeta^n, \quad \text{with } c_n = \sum_{i=0}^{\min(n,k)} \sum_{l=0}^{n-i} \binom{k}{i} \binom{l+k-1}{l} \left(\frac{\alpha}{\gamma}\right)^i \beta^l.$$

818 From this we can identify the error bound

$$819 \quad (A.28) \quad \boxed{\text{(PBI-Full)} : \quad e_{n+1}^k \leq \delta \gamma^k \sum_{i=0}^{\min(n,k)} \sum_{l=0}^{n-i} \binom{k}{i} \binom{l+k-1}{l} \left(\frac{\alpha}{\gamma}\right)^i \beta^l.}$$

820

REFERENCES

- 821 [1] E. AUBANEL, *Scheduling of tasks in the Parareal algorithm*, Parallel Comput., 37 (2011),
822 pp. 172–182.
- 823 [2] G. BAL, *On the convergence and the stability of the parareal algorithm to solve partial differ-*
824 *ential equations*, in Domain Decomposition Methods in Science and Engineering, R. Korn-
825 huber and et al., eds., vol. 40 of Lecture Notes in Computational Science and Engineering,
826 Berlin, 2005, Springer, pp. 426–432.
- 827 [3] M. BOLTEN, D. MOSER, AND R. SPECK, *A multigrid perspective on the parallel full approxima-*
828 *tion scheme in space and time*, Numerical Linear Algebra with Applications, 24 (2017),
829 p. e2110.
- 830 [4] M. BOLTEN, D. MOSER, AND R. SPECK, *Asymptotic convergence of the parallel full approx-*
831 *imation scheme in space and time for linear problems*, Numerical linear algebra with
832 applications, 25 (2018), p. e2208.
- 833 [5] J. BURMEISTER AND G. HORTON, *Time-parallel multigrid solution of the Navier-Stokes equa-*
834 *tions*, in Multigrid methods III, Springer, 1991, pp. 155–166.
- 835 [6] A. J. CHRISTLIEB, C. B. MACDONALD, AND B. W. ONG, *Parallel high-order integrators*, SIAM
836 J. Sci. Comput., 32 (2010), pp. 818–835.
- 837 [7] P.-H. COCQUET AND M. J. GANDER, *How large a shift is needed in the shifted Helmholtz pre-*
838 *conditioner for its effective inversion by multigrid?*, SIAM Journal on Scientific Computing,
839 39 (2017), pp. A438–A478.
- 840 [8] V. DOBREV, T. KOLEV, N. PETERSSON, AND J. SCHRODER, *Two-level convergence theory for*
841 *multigrid reduction in time (MGRIT)*, tech. report, LLNL-JRNL-692418, 2016.
- 842 [9] A. DUTT, L. GREENGARD, AND V. ROKHLIN, *Spectral deferred correction methods for ordinary*
843 *differential equations*, BIT, 40 (2000), pp. 241–266.
- 844 [10] H. C. ELMAN, O. G. ERNST, AND D. P. O’LEARY, *A multigrid method enhanced by Krylov*
845 *subspace iteration for discrete Helmholtz equations*, SIAM Journal on scientific computing,
846 23 (2001), pp. 1291–1315.
- 847 [11] M. EMMETT AND M. MINION, *Toward an efficient parallel in time method for partial differential*
848 *equations*, Comm. App. Math. and Comp. Sci., 7 (2012), pp. 105–132.
- 849 [12] O. G. ERNST AND M. J. GANDER, *Why it is difficult to solve Helmholtz problems with classical*
850 *iterative methods*, in Numerical analysis of multiscale problems, Springer, 2012, pp. 325–
851 363.
- 852 [13] O. G. ERNST AND M. J. GANDER, *Multigrid methods for Helmholtz problems: A convergent*
853 *scheme in 1d using standard components*, Direct and Inverse Problems in Wave Propaga-
854 tion and Applications, 14 (2013).
- 855 [14] R. D. FALGOUT, S. FRIEDHOFF, T. V. KOLEV, S. P. MACLACHLAN, AND J. B. SCHRODER,
856 *Parallel time integration with multigrid*, SIAM J. Sci. Comput., 36 (2014), pp. C635–C661.
- 857 [15] C. FARHAT AND M. CHANDESRIS, *Time-decomposed parallel time-integrators: theory and fea-*
858 *sibility studies for fluid, structure, and fluid-structure applications*, International Journal
859 for Numerical Methods in Engineering, 58 (2003), pp. 1397–1434.

- 860 [16] S. FRIEDHOFF, R. FALGOUT, T. KOLEV, S. MACLACHLAN, AND J. SCHRODER, *A multigrid-in-*
861 *time algorithm for solving evolution equations in parallel*, in Sixteenth Copper Mountain
862 Conference on Multigrid Methods, Copper Mountain, CO, United States, 2013.
- 863 [17] M. J. GANDER, *Analysis of the Parareal algorithm applied to hyperbolic problems using char-*
864 *acteristics*, Bol. Soc. Esp. Mat. Apl., 42 (2008), pp. 21–35.
- 865 [18] M. J. GANDER, *50 years of time parallel time integration*, in Multiple Shooting and Time
866 Domain Decomposition Methods, T. Carraro, M. Geiger, S. Körkel, and R. Rannacher,
867 eds., Springer, 2015, pp. 69–114.
- 868 [19] M. J. GANDER, I. G. GRAHAM, AND E. A. SPENCE, *Applying GMRES to the Helmholtz equation*
869 *with shifted Laplacian preconditioning: what is the largest shift for which wavenumber-*
870 *independent convergence is guaranteed?*, Numerische Mathematik, 131 (2015), pp. 567–
871 614.
- 872 [20] M. J. GANDER AND S. GÜTTEL, *ParaExp: A parallel integrator for linear initial-value problems*,
873 SIAM J. Sci. Comput., 35 (2013), pp. C123–C142.
- 874 [21] M. J. GANDER AND E. HAIRER, *Nonlinear convergence analysis for the Parareal algorithm*, in
875 Domain Decomposition Methods in Science and Engineering, Lecture Notes in Computa-
876 tional Science and Engineering, O. B. Widlund and D. E. Keyes, eds., vol. 60, Springer,
877 2008, pp. 45–56.
- 878 [22] M. J. GANDER, F. KWOK, AND H. ZHANG, *Multigrid interpretations of the Parareal algorithm*
879 *leading to an overlapping variant and MGRIT*, Computing and Visualization in Science,
880 19 (2018), pp. 59–74.
- 881 [23] M. J. GANDER AND T. LUNET, *Toward error estimates for general space-time discretizations*
882 *of the advection equation*, Comput. Vis. Sci., 23 (2020), pp. 1–14.
- 883 [24] M. J. GANDER AND T. LUNET, *ParaStieltjes: Parallel computation of Gauss quadrature rules*
884 *using a Parareal-like approach for the Stieltjes procedure*, Numerical Linear Algebra with
885 Applications, 28 (2021), p. e2314.
- 886 [25] M. J. GANDER AND M. NEUMULLER, *Analysis of a new space-time parallel multigrid algorithm*
887 *for parabolic problems*, SIAM Journal on Scientific Computing, 38 (2016), pp. A2173–
888 A2208.
- 889 [26] M. J. GANDER AND S. VANDEWALLE, *Analysis of the Parareal time-parallel time-integration*
890 *method*, SIAM J. Sci. Comput., 29 (2007), pp. 556–578.
- 891 [27] W. GAUTSCHI, *Orthogonal polynomials: computation and approximation*, Oxford University
892 Press, 2004.
- 893 [28] S. GÖTSCHEL, M. MINION, D. RUPRECHT, AND R. SPECK, *Twelve ways to fool the masses*
894 *when giving parallel-in-time results*, in Springer Proceedings in Mathematics & Statistics,
895 Springer International Publishing, 2021, pp. 81–94.
- 896 [29] S. GUNTHER, L. RUTHOTTO, J. B. SCHRODER, E. C. CYR, AND N. R. GAUGER, *Layer-parallel*
897 *training of deep residual neural networks*, SIAM Journal on Mathematics of Data Science,
898 2 (2020), pp. 1–23.
- 899 [30] W. HACKBUSCH, *Parabolic multi-grid methods*, in Proc. of the sixth int’l. symposium on Com-
900 puting methods in applied sciences and engineering, VI, North-Holland Publishing Co.,
901 1984, pp. 189–197.
- 902 [31] W. HACKBUSCH, *Multi-grid methods and applications*, vol. 4, Springer Science & Business
903 Media, 2013.
- 904 [32] A. HESSENTHALER, B. S. SOUTHWORTH, D. NORDSLETEN, O. RÖHRLE, R. D. FALGOUT, AND
905 J. B. SCHRODER, *Multilevel convergence analysis of multigrid-reduction-in-time*, SIAM
906 Journal on Scientific Computing, 42 (2020), pp. A771–A796.
- 907 [33] C. HOFER, U. LANGER, M. NEUMÜLLER, AND R. SCHNECKENLEITNER, *Parallel and robust pre-*
908 *conditioning for space-time isogeometric analysis of parabolic evolution problems*, SIAM
909 Journal on Scientific Computing, 41 (2019), pp. A1793–A1821.
- 910 [34] D. E. KNUTH, *The art of computer programming. 1. Fundamental algorithms*, Addison-Wesley,
911 1975.
- 912 [35] M. LECOUCVEZ, R. D. FALGOUT, C. S. WOODWARD, AND P. TOP, *A parallel multigrid reduc-*
913 *tion in time method for power systems*, in Power and Energy Society General Meeting
914 (PESGM), 2016, IEEE, 2016, pp. 1–5.
- 915 [36] J.-L. LIONS, Y. MADAY, AND G. TURINICI, *A "Parareal" in time discretization of PDE's*, C.
916 R. Math. Acad. Sci. Paris, 332 (2001), pp. 661–668.
- 917 [37] T. LUNET, J. BODART, S. GRATTON, AND X. VASSEUR, *Time-parallel simulation of the decay*
918 *of homogeneous turbulence using Parareal with spatial coarsening*, Computing and Visu-
919 alization in Science, 19 (2018), pp. 31–44.
- 920 [38] Y. MADAY AND E. M. RÖNQUIST, *Parallelization in time through tensor-product space-time*
921 *solvers*, Comptes Rendus Mathematique, 346 (2008), pp. 113–118.

- 922 [39] M. L. MINION, R. SPECK, M. BOLTEN, M. EMMETT, AND D. RUPRECHT, *Interweaving PFASST*
923 *and parallel multigrid*, SIAM J. Sci. Comput., 37 (2015), pp. S244–S263.
- 924 [40] S. MURATA, N. SATOFUKA, AND T. KUSHIYAMA, *Parabolic multi-grid method for incompressible*
925 *viscous flows using a group explicit relaxation scheme*, Computers & Fluids, 19 (1991),
926 pp. 33–41.
- 927 [41] B. W. ONG AND J. B. SCHRODER, *Applications of time parallelization*, Computing and Visual-
928 ization in Science, 23 (2020).
- 929 [42] E. M. RØNQUIST AND A. T. PATERA, *Spectral element multigrid. i. formulation and numerical*
930 *results*, Journal of Scientific Computing, 2 (1987), pp. 389–406.
- 931 [43] D. RUPRECHT, *Wave propagation characteristics of parareal*, Computing and Visualization in
932 Science, 19 (2018), pp. 1–17.
- 933 [44] D. RUPRECHT AND R. KRAUSE, *Explicit parallel-in-time integration of a linear acoustic-*
934 *advection system*, Comput. & Fluids, 59 (2012), pp. 72–83.
- 935 [45] D. RUPRECHT AND R. SPECK, *Spectral deferred corrections with fast-wave slow-wave splitting*,
936 SIAM Journal on Scientific Computing, 38 (2016), pp. A2535–A2557.
- 937 [46] M. SCHREIBER, P. S. PEIXOTO, T. HAUT, AND B. WINGATE, *Beyond spatial scalability limita-*
938 *tions with a massively parallel method for linear oscillatory problems*, The International
939 Journal of High Performance Computing Applications, 32 (2018), pp. 913–933.
- 940 [47] B. S. SOUTHWORTH, *Necessary conditions and tight two-level convergence bounds for Parareal*
941 *and multigrid reduction in time*, SIAM Journal on Matrix Analysis and Applications, 40
942 (2019), pp. 564–608.
- 943 [48] R. SPECK, D. RUPRECHT, R. KRAUSE, M. EMMETT, M. L. MINION, M. WINKEL, AND P. GIB-
944 BON, *A massively space-time parallel N-body solver*, in Proceedings of the International
945 Conference on High Performance Computing, Networking, Storage and Analysis, SC '12,
946 Los Alamitos, CA, USA, 2012, IEEE Computer Society Press, pp. 92:1–92:11.
- 947 [49] G. A. STAFF AND E. M. RØNQUIST, *Stability of the Parareal algorithm*, in Domain Decom-
948 position Methods in Science and Engineering, Lecture Notes in Computational Science and
949 Engineering, R. Kornhuber and et al, eds., vol. 40, Springer, 2005, pp. 449–456.
- 950 [50] U. TROTTENBERG, C. W. OOSTERLEE, AND A. SCHÜLLER, *Multigrid*, Academic Press Inc.,
951 New-York, 2001.
- 952 [51] G. WANNER AND E. HAIRER, *Solving ordinary differential equations II*, Springer Berlin Heidel-
953 berg, 1996.